Article

C#H Bond Activation of Heteroarenes Mediated by a Half-Sandwich Iron Complex of N-Heterocyclic Carbene

Yasuhiro Ohki, Tsubasa Hatanaka, and Kazuyuki Tatsumi

J. Am. Chem. Soc., **2008**, 130 (50), 17174-17186 • DOI: 10.1021/ja8063028 • Publication Date (Web): 14 November 2008

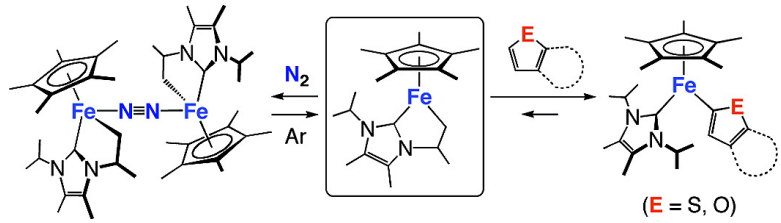

More About This Article

Additional resources and features associated with this article are available within the HTML version:

- Supporting Information
- Access to high resolution figures
- Links to articles and content related to this article
- Copyright permission to reproduce figures and/or text from this article

View the Full Text HTML

J|A|C|S
ARTICLES

Published on Web 11/14/2008

C−H Bond Activation of Heteroarenes Mediated by a Half-Sandwich Iron Complex of N-Heterocyclic Carbene

Yasuhiro Ohki,* Tsubasa Hatanaka, and Kazuyuki Tatsumi*

Department of Chemistry, Graduate School of Science, and Research Center for Meterials Science, Nagoya University, Furo-cho, Chikusa-ku, Nagoya 464-8602, Japan

Received August 9, 2008

E-mail: i45100a@nucc.cc.nagoya-u.ac.jp (K. T.); ohki@mbox.chem.nagoya-u.ac.jp (Y. O.)

Abstract: Half-sandwich iron complexes of N-heterocyclic carbenes, Cp*Fe(L^R)Cl (**2a**; L^{Mes} = 1,3-dimesityl-imidazol-2-ylidene, **2b**; L^{iPr} = 1,3-diisopropyl-4,5-dimethylimidazol-2-ylidene, Cp* = η^5-C_5Me_5), have been synthesized by the reaction of Cp*Fe{$N(SiMe_3)_2$} (**1**) with the corresponding imidazolium salts. Treatment of **2a** with either methyllithium or phenyllithium replaces the chloride with either a methyl or a phenyl group, generating Cp*Fe(L^{Mes})R (**3a**; R = Me, **3b**; R = Ph). These complexes, in turn, undergo cyclometalation at elevated temperatures, and Cp*Fe{κ^2-(C,C)-L'^{Mes}} (**4**; L'^{Mes} = $CH_2C_6H_2$-3,5-Me_2-2-(3-mesityl-imidazol-2-ylidene-1-yl)) was isolated. On the other hand, methylation of **2b** at room temperature leads directly to the formation of a cyclometalated complex, Cp*Fe{κ^2-(C,C)-L'^{iPr}} (**6**; L'^{iPr} = $CH_2CH(CH_3)$(3-isopropyl-4,5-dimethylimidazol-2-ylidene-1-yl)). The Fe(II) center of **6** traps atmospheric dinitrogen reversibly to produce a dinuclear end-on N_2 complex [Cp*Fe{κ^2-(C,C)-L'^{iPr}}]$_2$(μ-η^1:η^1-N_2) (**7**). Complex **6** also promotes C−H bond activation of thiophene, furan, benzothiophene, and benzofuran at room temperature. In these reactions, C−H bond cleavage occurred exclusively at the 2-position of the rings, generating Cp*Fe(L^{iPr})(2-C_4H_3E) (**8**; E = S, **9**; E = O) and Cp*Fe(L^{iPr})(2-C_8H_5E) (**10**; *E* = S, **11**; *E* = O), while C−H cleavage took place mainly at the 4-position in the case of pyridine. Coupling reactions between heteroarenes and catecholborane (HBcat) can be carried out by treatment of **6** with heteroarenes followed by the addition of excess HBcat, giving rise to 2-boryl-heteroarenes and the borohydride complex Cp*Fe(L^{iPr})(H_2Bcat) (**14**).

Introduction

The activation of C−H bonds is a key elementary step of organometallic reactions, and has great utility in organic synthesis.[1] Whereas there have been a number of examples of C−H bond cleavage promoted by transition metal complexes, either stoichiometric or catalytic, noble metal elements have been used in most cases.[1,2] Recently, the importance of iron, highly abundant and with low toxicity, has been recognized for the activation and transformation of organic/inorganic substrates.[3] In the late 1970s, Tolman and Ittel et al. reported early work on C−H bond cleavage by a transient 16-electron Fe(0) species, Fe(dmpe)$_2$, which was generated by reductive elimination of naphthalene from Fe(dmpe)$_2$(Np)H (Np = 2-naphthyl, dmpe = bis(dimethylphosphino)ethane).[4] Later, photolysis of Fe(dmpe)$_2$H$_2$ was found to to activate C−H bonds of alkenes via generation of the same transient species, Fe(dmpe)$_2$.[5] The catalytic insertion of isocyanide into aromatic C−H bonds was attained by irradiation of Fe$(CNR)_3(PMe_3)_2$ (R = Me, ^{t}Bu, CH_2CMe_3, Ph, 2,6-xylyl),[6] while the photochemical reactions of Cp*Fe$(CO)_2$(Bcat′) (Cp* = η^5-C_5Me_5; cat′ = 1,2-$O_2C_6H_2$-3,5-Me_2) with alkanes induced borylation at the terminal C−H position.[7] Apparently, the preparation of a coordinatively unsaturated iron complex is a prerequisite for successful C−H bond activation under mild conditions. Herein we report the activation of C−H bonds of thiophenes, furans, and pyridine, promoted by a coordinatively unsaturated half-sandwich iron complex containing a metallacycle derived from an N-heterocyclic carbene (L^R). Furthermore, treatment of this unsaturated iron complex with thiophene, furan, benzothiophene, or benzofuran followed by addition of catecholborane (HBcat), was

(1) (a) Shilov, A. E.; Shul'pin, G. B. *Chem. Rev.* **1997**, *97*, 2879–2932. (b) Dyker, G. *Angew. Chem., Int. Ed.* **1999**, *38*, 1698–1712. (c) Jia, C.; Kitamura, T.; Fujiwara, Y. *Acc. Chem. Res.* **2001**, *34*, 633–639. (d) Jun, C.-H.; Moon, C. W; Lee, D.-Y. *Chem.−Eur. J.* **2002**, *8*, 2422–2428. (e) Ritleng, V.; Sirlin, C.; Pfeffer, M. *Chem. Rev.* **2002**, *102*, 1731–1769. (f) Kakiuchi, F.; Murai, S. *Acc. Chem. Res.* **2002**, *35*, 826–834. (g) Davies, H. M. L.; Beckwith, R. E. J. *Chem. Rev.* **2003**, *103*, 2861–2903. (h) Pamplin, G. B.; Legzdins, P. *Acc. Chem. Res.* **2003**, *36*, 223–233.

(2) (a) Naota, T.; Takaya, H.; Murahashi, S.-I. *Chem. Rev.* **1998**, *98*, 2599–2660. (b) Esteruelas, M. A.; López, A. M. *Organometallics* **2005**, *24*, 3584–3613. (c) Lersch, M.; Tilset, M. *Chem. Rev.* **2005**, *105*, 2471–2526. (d) Alberico, D.; Scott, M. E.; Lautens, M. *Chem. Rev.* **2007**, *107*, 174–238.

(3) Bolm, C.; Legros, J.; Le Paih, J.; Zani, L. *Chem. Rev.* **2004**, *104*, 6217–6254.

(4) (a) Tolman, C. A.; Ittel, S. D.; English, A. D.; Jesson, J. P. *J. Am. Chem. Soc.* **1978**, *100*, 4080–4089. (b) Ittel, S. D.; Tolman, C. A.; English, A. D.; Jesson, J. P. *J. Am. Chem. Soc.* **1978**, *100*, 7577–7585. (c) Tolman, C. A.; Ittel, S. D.; English, A. D.; Jesson, J. P. *J. Am. Chem. Soc.* **1979**, *101*, 1742–1751.

(5) Baker, M. V.; Field, L. D. *J. Am. Chem. Soc.* **1986**, *108*, 7433–7434.

(6) Jones, W. D.; Foster, G. P.; Putinas, J. M. *J. Am. Chem. Soc.* **1987**, *109*, 5047–5048.

(7) (a) Waltz, K. M.; Hartwig, J. F. *Science* **1997**, *277*, 211–213. (b) Waltz, K. M.; Hartwig, J. F. *J. Am. Chem. Soc.* **2000**, *122*, 11358–11369. (c) Webster, C. E.; Fan, Y.; Hall, M. B.; Kunz, D.; Hartwig, J. F. *J. Am. Chem. Soc.* **2003**, *125*, 858–859.

10.1021/ja8063028 CCC: $40.75

Scheme 1

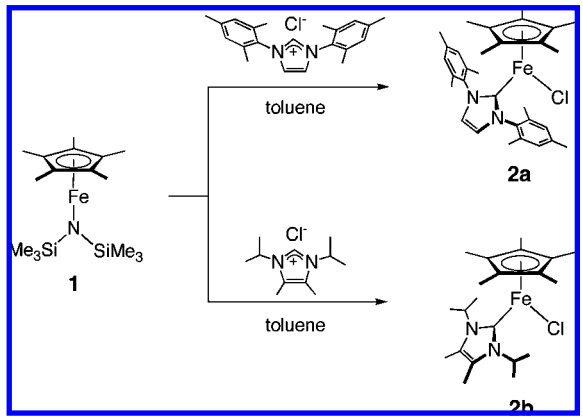

found to produce 2-boryl-heteroarenes and an iron-borohydride complex via sequential C−H bond activation and borylation reactions.

Results and Discussion

Synthesis and Structures of Cp*Fe(L^R)Cl. We have recently demonstrated that the amide ligand in Cp*Fe{N(SiMe$_3$)$_2$} (**1**)[8] acts as a Brønsted base and deprotonates methylaniline and 1,2-diphenylhydrazine to give (Cp*Fe)$_2$(μ-NMePh)$_2$ and (Cp*Fe)$_2$(μ-NPh)$_2$, respectively.[9] Also Fe{N(SiMe$_3$)$_2$}$_2$[10] can be used to deprotonate bulky arylthiols to generate a series of low-coordinate iron complexes[11] and to produce intriguing Fe/S/SAr clusters which model the active sites of nitrogenase.[12] Here we report the synthesis of half-sandwich iron complexes of N-heterocyclic carbenes following a similar line, using the acid−base reaction of **1** with imidazolium salts.

Treatment of a toluene solution of **1** with the imidazolium salt (HL^{Mes})(Cl) (L^{Mes} = 1,3-dimesityl-imidazol-2-ylidene)[13] at −78 °C resulted in the formation of a brownish green solution, from which crystals of Cp*Fe(L^{Mes})Cl (**2a**) were isolated in 92% yield. The analogous complex with L^{iPr} (1,3-diisopropyl-4,5-dimethylimidazol-2-ylidene),[13] Cp*Fe(L^{iPr})Cl (**2b**), was obtained similarly as dark green crystals in 69% yield (Scheme 1). These carbene complexes **2a** and **2b** are highly sensitive to air/moisture and need to be handled under inert conditions. However, they are thermally stable in solution and decompose only gradually over several days in boiling C_6D_6. According to the ^{1}H NMR spectra of **2a** and **2b**, the compounds are paramagnetic, revealing significant paramagnetic shifts of the Cp* and carbene protons. For instance, the Cp* resonance appears at δ 169 (**2a**) and 120 (**2b**), and the three mesityl-CH$_3$ signals for **2a** were observed at δ 76.0, −11.4, and −43.6. Hindered rotation of the mesityl groups of **2a** is indicated by the inequivalence of the three CH$_3$ signals of each mesityl subsituent.

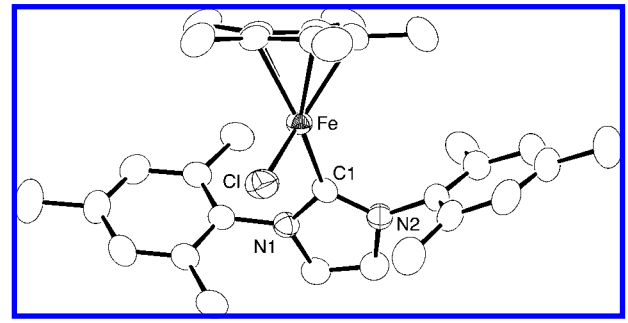

Figure 1. Molecular structure of **2a** with thermal ellipsoids at the 50% probability level. Selected bond distances (Å) and angles (deg) for **2a** and **2b**: **2a**, Fe−Cl = 2.2715(7), Fe−C(1) = 2.085(3), C(1)−N(1) = 1.361(3), C(1)−N(2) = 1.364(3), Cl−Fe−C(1) = 98.14(7), N(1)−C(1)−N(2) = 103.3(2). **2b**, Fe−Cl = 2.2434(8), Fe−C(1) = 1.950(2), C(1)−N(1) = 1.366(2), C(1)−N(2) = 1.358(2), Cl−Fe−C(1) = 95.46(6), N(1)−C(1)−N(2) = 104.64(17).

Single crystals of **2a** and **2b** suitable for X-ray diffraction were grown from concentrated Et$_2$O solutions. Their molecular structures are very similar, and Figure 1 shows only an ORTEP drawing of **2a**, while selected bond distances and angles for **2a** and **2b** are given in the figure caption. These are coordinatively unsaturated half-sandwich 16e complexes, and the Fe−Cl distances of **2a** and **2b** are shorter by 0.02−0.10 Å than those of analogous 18e complexes of iron.[14] While numerous half-sandwich iron complexes have been crystallographically characterized, those with 16 electrons are still limited.[15] We propose that the bulky carbene ligands (L^R) kinetically stabilize the electron-deficient iron center. The Fe−C(carbene) bond length appears to vary depending upon the steric bulk of the substituent. The Fe−C(L^{Mes}) bond of **2a** is notably longer (by 0.135(3) Å) compared with the Fe−C(L^{iPr}) bond of **2b**, and it is also longer than previously reported Fe(II)-L$^{R'}$ (R′ = ^{i}Pr, Mes) bonds with less bulky ligands on iron (1.933(8)−1.980(5) Å).[16] In both **2a** and **2b**, the iron atom sits in the plane defined by the centroid of Cp*, the carbene carbon, and the Cl, and the five-member ring of L^R is situated nearly perpendicular to this plane. These interplane angles are 76.59(8)° for **2a** and 89.18(6)° for **2b**. The two mesityl aromatic rings of L^{Mes} in **2a** orient nearly perpendicular to the N-heterocyclic ring with interplane angles of 78.3(1) and 79.4(1)°. Given the geometry of Cp*FeCl(L^R), we envisage the d-orbital splitting to be as depicted in Scheme 2. The middle two orbitals, $x^2 - y^2$ and yz each accommodate an unpaired electron, giving a triplet electronic state. If L^R is

(8) Siemeling, U.; Vorfeld, U.; Neumann, B.; Stammler, H.-G. *Organometallics,* **1998**, *17*, 483–484.
(9) Ohki, Y.; Takikawa, Y.; Hatanaka, T.; Tatsumi, K. *Organometallics* **2006**, *25*, 3111–3113.
(10) Andersen, R. A.; Faegri, K., Jr.; Green, J. C.; Haaland, A.; Lappert, M. F.; Leung, W.-P.; Rypdal, K. *Inorg. Chem.* **1988**, *27*, 1782–1786.
(11) (a) Ellison, J. J.; Ruhlandt-Senge, K.; Power, P. P. *Angew. Chem., Int. Ed. Engl.* **1994**, *33*, 1178–1180. (b) Hauptmann, R.; Kliβ, R.; Schneider, J.; Henkel, G. *Z. Anorg. Allg. Chem.* **1998**, *624*, 1927–1936. (c) Komuro, T.; Kawaguchi, H.; Tatsumi, K. *Inorg. Chem.* **2002**, *41*, 5083–5090. (d) Ohta, S.; Ohki, Y.; Ikagawa, Y.; Suizu, R.; Tatsumi, K. *J. Organomet. Chem.* **2007**, *692*, 4792–4799.
(12) (a) Ohki, Y.; Sunada, Y.; Honda, M.; Katada, M.; Tatsumi, K. *J. Am. Chem. Soc.* **2003**, *125*, 4052–4053. (b) Ohki, Y.; Sunada, Y.; Tatsumi, K. *Chem. Lett.* **2005**, *34*, 172–173. (c) Ohki, Y.; Ikagawa, Y.; Tatsumi, K. *J. Am. Chem. Soc.* **2007**, *129*, 10457–10465.
(13) (a) Kuhn, N.; Kratz, T. *Synthesis* **1993**, 561–562. (b) Arduengo, A. J., III; Krafczyk, R.; Schmutzler, R. *Tetrahedron* **1999**, *55*, 14523–14534.
(14) (a) Clegg, W.; Compton, N. A.; Errington, J.; Norman, N. C. *J. Chem. Soc., Dalton Trans.* **1988**, 1671–1678. (b) Roger, C.; Hamon, P.; Toupet, L.; Rabaa, H.; Saillard, J.-Y.; Hamon, J.-R.; Lapinte, C. *Organometallics* **1991**, *10*, 1045–1054. (c) Akita, M.; Terada, M.; Tanaka, M.; Moro-oka, Y. *J. Organomet. Chem.* **1996**, *510*, 255–261. (d) Tilset, M.; Fjeldahl, I.; Hamon, J.-R.; Hamon, P.; Toupet, L.; Saillard, J.-Y.; Costuas, K.; Haynes, A. *J. Am. Chem. Soc.* **2001**, *123*, 9984–10000. (e) Shneider, J. J.; Spickermann, D.; Lehmann, C. W.; Magull, J.; Krüger, H.-J.; Ensling, J.; Gütlich, P. *Chem.−Eur. J.* **2006**, *12*, 1427–1435.
(15) (a) Sapunov, V. N.; Schmid, R.; Kirchner, K.; Nagashima, H. *Coord. Chem. Rev.* **2003**, *238−239*, 363–382. (b) Jiménez-Tenorio, M.; Puerta, M. C.; Valerga, P. *Eur. J. Inorg. Chm.* **2004**, *17−32*.
(16) (a) Buchgraber, P.; Toupet, L.; Guerchais, V. *Organometallics* **2003**, *22*, 5144–5147. (b) Danopoulos, A. A.; Tsoureas, N.; Wright, J. A.; Light, M. E. *Organometallics* **2004**, *23*, 166–168. (c) McGuinness, D. S.; Gibson, V. C.; Steed, J. W. *Organometallics* **2004**, *23*, 6288–6292.

Scheme 2

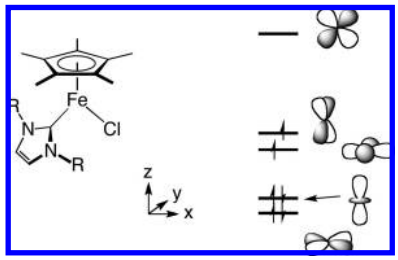

Scheme 3

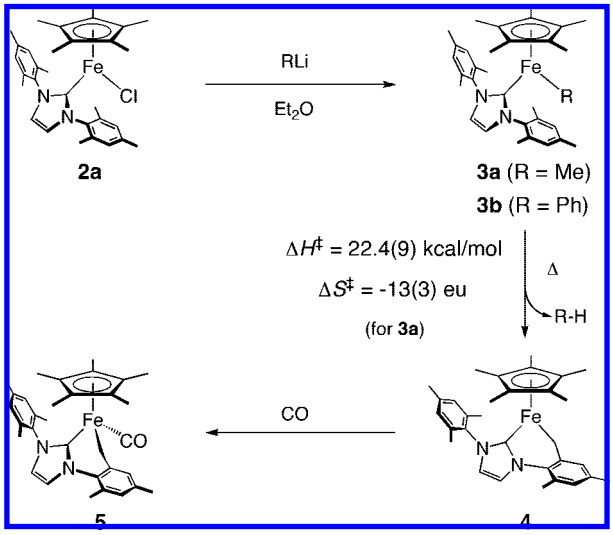

considered to donate two σ-electrons to Fe(II), the carbene carbon p_π orbital is formally vacant. Thus, a Fe−C(L^R) p_π−d_π interaction would occur with the occupied z^2 orbital, providing there is a double bond character in the bond. When the N-heterocyclic carbene ligand rotates along the Fe−C(L^{Mes}) bond by 90°, the C(L^R) p_π orbital can now interact with the occupied *xy* orbital, instead of z^2. Therefore, the rotational barrier should not be prohibitively high.

Synthesis of Cp*Fe(L^{Mes})Me and Cp*Fe(L^{Mes})Ph and Intramolecular C−H Bond Activation. Addition of an ether solution of MeLi to **2a** in the same solvent at −78 °C did not produce a noticeable color change. However, when the temperature was raised to ca. 0 °C, the color turned gradually from dark green to orange, and a white powder precipitated. Cp*Fe(L^{Mes})Me (**3a**) was isolated in 84% yield as orange crystals after recrystallization from hexane. A similar treatment of **2a** with PhLi, produced orange crystals of Cp*Fe(L^{Mes})Ph (**3b**) in 77% yield (Scheme 3). Similarly to **2a**, the ^{1}H NMR spectra show paramagnetically broadened and shifted signals. Again, there appear three signals for the methyl groups of L^{Mes} at δ 32.3, −3.9, −30.4 for **3a**, and at δ 28.5, −0.7, −28.6 for **3b**. The Fe−CH_3 signal of **3a**, shifted substantially, is found at δ −458.

The molecular structures of **3a** and **3b** were determined by X-ray analysis of crystals grown from hexane. Figure 2 shows an ORTEP view of **3b**, and selected bond distances and angles for **3a** and **3b** are given in the caption. The structures of **3a** and **3b** are very similar to that of **2a**, except for the orientation of L^{Mes} group and the Fe−C(L^{Mes}) bond lengths. The carbene ligand rotates around the Fe−C(L^{Mes}) bond from the "perpendicular" orientation, and the interplane angle between the N-heterocyclic ring and the mean plane of Fe, C(L^{Mes}), C(Me or Ph), and

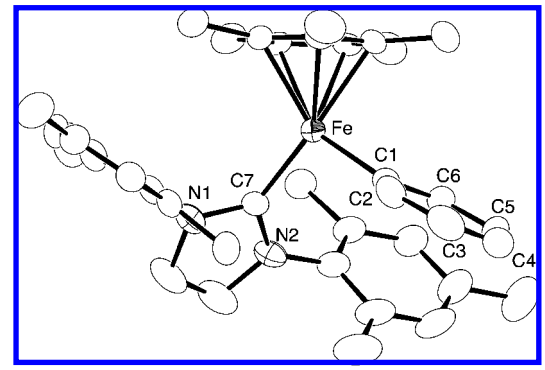

Figure 2. Molecular structure of **3b** with thermal ellipsoids at the 50% probability level. Selected bond distances (Å) and angles (deg) for **3a** and **3b**: **3a**, Fe−C(1) = 2.009(2), Fe−C(2) = 1.931(2), C(2)−N(1) = 1.371(2), C(2)−N(2) = 1.384(3), C(1)−Fe−C(2) = 90.51(9), N(1)−C(2)−N(2) = 102.3(2). **3b**, Fe−C(1) = 1.982(2), Fe−C(7) = 1.968(2), C(7)−N(1) = 1.386(4), C(7)−N(2) = 1.381(4), C(1)−Fe−C(7) = 100.29(11), N(1)−C(7)−N(2) = 102.0(2).

Cp*(centroid) is 66.29(9)° for **3a** or 64.3(1)° for **3b**. Interestingly, the Fe−C(L^{Mes}) bonds of **3a** and **3b** are both notably shorter than that of **2a**.

Although **3a** and **3b** are thermally stable in solution at ambient temperature, it was found that the color of a C_6D_6 solution of **3a** in an NMR tube gradually turned from orange to dark green at 60 °C over a three-day period. The ^{1}H NMR spectrum indicated the formation of methane and a new paramagnetic species. Thermolysis of **3b** in C_6D_6 also proceeded slowly at 60 °C, and the same paramagnetic compound was detected by ^{1}H NMR after four days. This paramagnetic species was isolated as dark green thin plates in 81% yield. Although the quality of the X-ray data was not high, it was possible to formulate the product as Cp*Fe{κ^2-(C,C)-L′^{Mes}} (**4**; L′^{Mes} = $CH_2C_6H_2$-3,5-Me_2-2-(3-mesityl-imidazol-2-ylidene-1-yl)) (see Supporting Information). The thermal reaction of **3a** or **3b** thus induced cyclometalation of L^{Mes}, via intramolecular C−H bond activation of an ortho-Me (mesityl) group and subsequent liberation of methane or benzene. The ^{1}H NMR spectrum of **4** contains five broad signals assignable to mesityl-CH_3 protons at δ −1.7, −8.7, −11.9, −12.8, and −14.6, which are in accordance with the X-ray derived structure of **4**. On the other hand, signals for the methylene protons were not detected in the region between −500 ppm and +500 ppm.

Kinetic data for the transformation of **3a** into **4** were obtained by ^{1}H NMR (40∼80 °C, in C_6D_6), by monitoring the Cp* proton signal of **3a** using cyclohexane signal as an internal standard. The reaction was found to obey pseudofirst-order kinetics with respect to the concentration of **3a**, and the activation parameters from the Eyring plot shown in Figure 3 are $\Delta H^\ddagger$ = 22.4(9) kcal/mol and $\Delta S^\ddagger$ = −13(3) eu. The negative activation entropy is consistent with a transition state structure in which some bond rotational freedom is lost.

When a toluene solution of **4** was exposed to 1 atm CO at room temperature, an immediate color change from dark green to orange was noticed, and a diamagnetic 18e CO adduct, Cp*Fe{κ^2-(C,C)-L′^{Mes}}(CO) (**5**), was isolated as orange crystals in 53% yield. The ^{1}H NMR signals characteristic of iron-bound methylene protons appeared at δ 2.06 and 1.60, and the corresponding carbon resonance was observed at δ 8.9 in the ^{13}C{^{1}H} NMR spectrum. The CO stretching band at 1872 cm^{-1} in the IR spectrum is lower than those of the analogous complexes CpFe(L^{Mes})(CO)Me (1886 cm^{-1}) and CpFe(L^{Mes})-

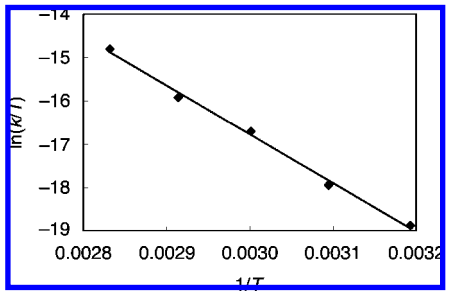

Figure 3. Eyring plot for the thermal conversion of **3a** into **4**. The activation parameters were determined as $\Delta H^{\ddagger} = 22.4(9)$ kcal/mol and $\Delta S^{\ddagger} = -13(3)$ eu.

Scheme 4

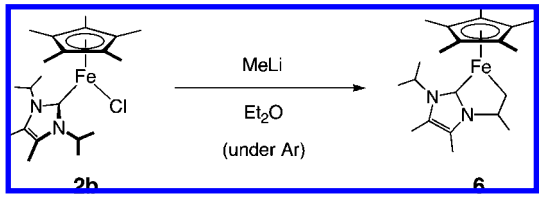

(CO)I (1938 cm^{-1}).[17] The molecular structure of **5** was determined by X-ray crystallography. Structural data can be found in the Supporting Information, and here we only mention that the Fe−C bond distance for the cyclometalated methylene is 2.063(2) Å, which is comparable to the Fe−C(alkyl) distances found in Cp*Fe(CO)$_2$R (2.057(3)−2.146(10) Å, R = C_3H_7, C_3H_6Br, CH_2SiMe_2OH, $(CH_2)_4OSiMe_2NPh_2$, η^1-C_5H_5).[18]

Reaction of Cp*Fe(L^{iPr})Cl with Methyllithium. Methylation of **2b**, Cp*Fe(L^{iPr})Cl, was also examined. Addition of methyllithium to an ether solution of **2b** at −78 °C first gave an orange solution with precipitation of a white solid. In contrast to the analogous reaction of **2a**, a further color change to yellowish brown occurred gradually at room temperature, from which Cp*Fe{κ^2-(C,C)-L′^{iPr}} (**6**; L′^{iPr} = $CH_2CH(CH_3)$(3-isopropyl-4,5-dimethylimidazol-2-ylidene-1-yl)) was isolated in 98% yield as crystals (Scheme 4). Although isolation of Cp*Fe(L^{iPr})Me was not possible, in view of the initial orange color, which is similar to the color of Cp*Fe(L^{Mes})Me (**3a**), it is a likely precursor which undergoes intramolecular C−H bond activation to give **6**. The decreased thermal stability of Cp*Fe(L^{iPr})Me relative to **3a** may be due to the less bulky ^{i}Pr substituent of the carbene.

The molecular structure of **6** was determined by X-ray diffraction. The cyclometalated L′^{iPr} ligand and Cp* are disordered over two positions with 50:50 occupancy, and for clarity only one component is shown in Figure 4. The Fe−C(carbene) distance of 1.949(3) Å is close to that of **2b** (1.950(2) Å), and the Fe−C(methylene) distance (2.023(7) Å) is in the typical range of iron−alkyl bonds.[18] The bite angle of the L′^{iPr} ligand is 83.7(4)° and is more acute compared to those

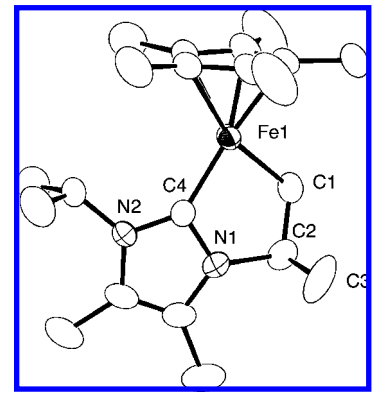

Figure 4. Molecular structure of **6** with thermal ellipsoids at the 50% probability level. The cyclometalated L′^{iPr} ligand and Fe are disordered over two positions with 50:50 occupancy, and for clarity only one component is shown. Selected bond distances (Å) and angles (deg): Fe−C(1) = 2.023(7), Fe(1)−C(4) = 1.949(3), C(1)−C(2) = 1.509(11), C(2)−N(1) = 1.563(9), C(4)−N(1) = 1.364(4), C(4)−N(2) = 1.354(4), C(4)−Fe−C(1) = 83.6(2), Fe−C(1)−C(2) = 111.0(5), N(1)−C(4)−Fe = 115.5(2), N(2)−C(4)−Fe = 140.4(2), N(1)−C(4)−N(2) = 102.7(2).

Scheme 5

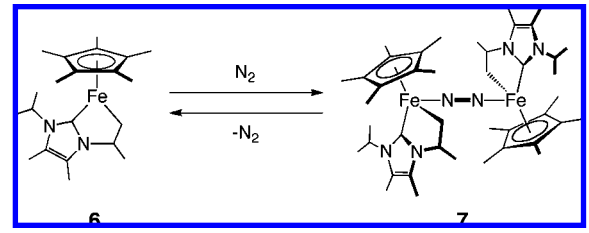

of the unsaturated diphosphine complexes [Cp*Fe(P^P)]$^+$ (86.5(2)−95.62(6)°; P^P = dippe, dppe, dppp).[19]

Formation of [Cp*Fe{κ^2-(C,C)-L′^{iPr}}]$_2$(μ-η^1:η^1-N$_2$). When a hexane solution of **6** stood under an N_2 atmosphere for one hour, red crystals of the dinuclear N_2 complex [Cp*Fe{κ^2-(C,C)-L′^{iPr}}]$_2$(μ-η^1:η^1-N$_2$) (**7**) formed (Scheme 5). An X-ray diffraction study of these crystals revealed the structure shown in Figure 5, where the iron has the coordination geometry of a three-legged piano-stool. The bridging N_2 ligand is bound in an end-on fashion with an Fe−N bond length of 1.8109(13) Å and an N−N distance of 1.1322(18) Å. These distances are comparable to those reported for Fe(II) complexes having a terminal N_2 ligand.[19a,20] The short N−N distance and the high ν_{N-N} stretching frequency of **7** (2126 cm^{-1}) observed in the Raman spectrum indicate weak coordination of N_2 at Fe and little decrease of N≡N triple bond character. Indeed, when red crystals of **7** are dissolved, the color of the solution quickly changes to the orange of **6**, and the characteristic paramagnetic ^{1}H NMR spectrum confirms that **7** is transformed into **6** upon dissolution. ^{1}H NMR shows a small diamagnetic signal, which may be a remaining small amount of **7** in equilibrium with **6**.

(17) (a) Buchgraber, P.; Toupet, L.; Guerchais, V. *Organometallics* **2003**, *22*, 5144–5147. (b) Llewellyn, S. A.; Green, M. L. H.; Green, J. C.; Cowley, A. R. *Dalton Trans.* **2006**, 2535–2541.

(18) (a) Wright, M. E.; Nelson, G. O.; Glass, R. S. *Organometallics* **1985**, *4*, 245–250. (b) Hill, R. O.; Marais, C. F.; Moss, J. R.; Naidoo, K. J. *J. Organomet. Chem.* **1999**, *587*, 28–37. (c) Malisch, W.; Hofmann, M.; Nieger, M.; Schöller, W. W.; Sundermann, A. *Eur. J. Inorg. Chem.* **2002**, 3242–3252. (d) Okazaki, M.; Iwata, M.; Tobita, H.; Ogino, H. *Dalton Trans.* **2003**, 1114–1120. (e) Friedrich, H. B.; Onani, M. O.; Rademeyer, M. *Acta Cryst. E* **2004**, *60*, m551–m553.

(19) (a) de la Leal, A. J.; Tenorio, M. J.; Puerta, M. C.; Valerga, P *Organometallics* **1995**, *14*, 3839–3847. (b) Hamon, P.; Toupet, L.; Hamon, J.-R.; Lapinte, C. *Organometallics* **1996**, *15*, 10–12. (c) Argouarch, G.; Hamon, P.; Toupet, L.; Hamon, J.-R.; Lapinte, C. *Organometallics* **2002**, *21*, 1341–1348.

(20) (a) Hills, A.; Hughes, D. L.; Jimenez-Tenorio, M.; Leigh, G. J.; Rowley, A. T. *J. Chem. Soc., Dalton Trans.* **1993**, 3041–3049. (b) Buys, I. E.; Field, L. D.; Hambley, T. W.; McQueen, A. W. D. *Acta Cryst. C* **1993**, *49*, 1056–1059. (c) Wiesler, B. E.; Lehnert, N.; Tuczek, F.; Neuhausen, J.; Tremel, W. *Angew. Chem., Int. Ed.* **1998**, *37*, 815–817.

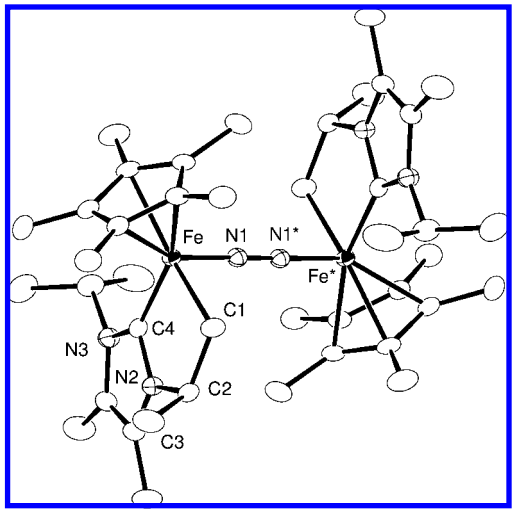

Figure 5. Molecular structure of **7** with thermal ellipsoids at the 50% probability level. Selected bond distances (Å) and angles (°): Fe−N(1) = 1.8109(13), N(1)−N(1)* = 1.1322(18), Fe−C(1) = 2.055(2), Fe−C(4) = 1.9345(15), C(1)−C(2) = 1.536(2), C(2)−N(2) = 1.467(2), N(2)−C(4) = 1.359(2),C(4)−N(3)=1.367(2),Fe−N(1)−N(1)*=176.80(14),C(1)−Fe−N(1) = 89.33(7), C(1)−Fe−C(4) = 80.67(7), C(4)−Fe−N(1) = 88.80(5), Fe−C(1)−C(2) = 113.80(11), Fe−C(4)−N(2) = 118.92(11), Fe−C(4)−N(3) = 136.54(14), N(2)−C(4)−N(3) = 103.68(14).

C−H Bond Activation of Thiophenes, Furans, and Pyridine. Complex **6**, which was generated by dissolving crystals of **7** in organic solvents (toluene, hexane, pentane, THF, or C_6D_6) under an argon atmosphere, was found to mediate C−H bond activation of thiophenes, furans, and pyridine, under mild conditions. The reaction of in situ generated **6** with thiophene occurred at room temperature to furnish brownish green crystals of the 2-thienyl complex Cp*Fe(L^{iPr})(2-C_4H_3S) (**8**) (Scheme 6). This complex forms via hydrogen atom transfer from the 2-position of thiophene to the methylene group of the L'^{iPr} ligand. In a similar manner, the reactions with furan, benzothiophene, and benzofuran gave the 2-heteroaryl complexes **9**−**11**, respectively. The iron centers in these complexes are formally 16e and thus unsaturated. Single crystals of **8**−**10** suitable for X-ray diffraction were grown from hexane (**8**), pentane (**9**), or toluene (**10**) solutions. The structure of **11** was also identified by preliminary X-ray analysis of crystals obtained from toluene (see Supporting Information). The solid-state structures of complexes **8** and **10** are shown in Figure 6, and selected bond distances and angles for **8**−**10** are provided in Table 1. The 2-thienyl complex **8** has crystallographic C_s symmetry, with the Fe, C(carbene), and the 2-thienyl group on the mirror plane. The heteroaryl groups in **9** and **10** are close to coplanar with the plane consisting of C(carbene)−Fe−C(heteroaryl), showing interplanar angles of 0.20(14) and 22.00(10)−23.80(12)°, respectively. Comparison of the Fe−C(heteroaryl) bond distances in **8**−**10** (1.945(3)−1.971(2) Å) to the Fe−C(methylene) distance found in **6** (2.023(7) Å) reveals a shortening by approximately 0.05−0.07 Å, which is consistent with the change in hybridization from Fe−C(sp^3) to Fe−C(sp^2). On the other hand, the Fe−C(carbene) bond length (1.949(3)−1.959(2) Å) remains unchanged.

Complexes **8**−**11** are paramagnetic and show significantly shifted ^{1}H NMR signals. The signals for Cp* and L^{iPr} in **8**−**11** are similar, with the Cp* resonances appearing in the range of δ 42.6−48.6 while the L^{iPr} group shows three methyl signals at δ 18.4−21.6, δ 6.8−8.5, and δ 3.0−7.2. It is notable that the ^{1}H NMR spectra of **8**−**11** exhibited small signals due to **6** and the liberated heteroarenes, in addition to the major signals for **8**−**11**, indicating an equilibrium between **6** + heteroarene and the 2-heteroaryl complex.

Pyridine also exhibited C−H bond cleavage mediated by **6** (Scheme 7). Addition of excess pyridine to a C_6D_6 solution of in situ generated **6** gave rise to new paramagnetic ^{1}H NMR signals, which are assignable to the pyridyl complex Cp*Fe(L^{iPr})(C_5H_4N) (**12**). The chemical shifts for Cp* at δ 47.7 and L^{iPr} at δ 23.4, 4.9, and 2.8 are close to those observed for compounds **8**-**11**. Whereas these signals are dominant in a solution of **6** with excess pyridine at room temperature, in the solid state only **6** could be obtained apparently due to the facile regeneration of **6** from the pyridyl complex. This facile and reversible hydrogen atom transfer between pyridine and the L^{iPr} ligand prompted us to explore the H/D scrambling reaction of **6** with pyridine-d_5. Interestingly, monitoring of a mixture of **6** and 200 equiv of pyridine-d_5 by ^{1}H NMR indicated that both the 4- and 2-positions of pyridine-d_5 underwent H/D exchange, leaving the 3-position almost intact (Figure 7). Thus the reaction mixture of **6** and pyridine likely contains both 4-pyridyl and 2-pyridyl complexes, although only one set of signals for Cp*

Scheme 6

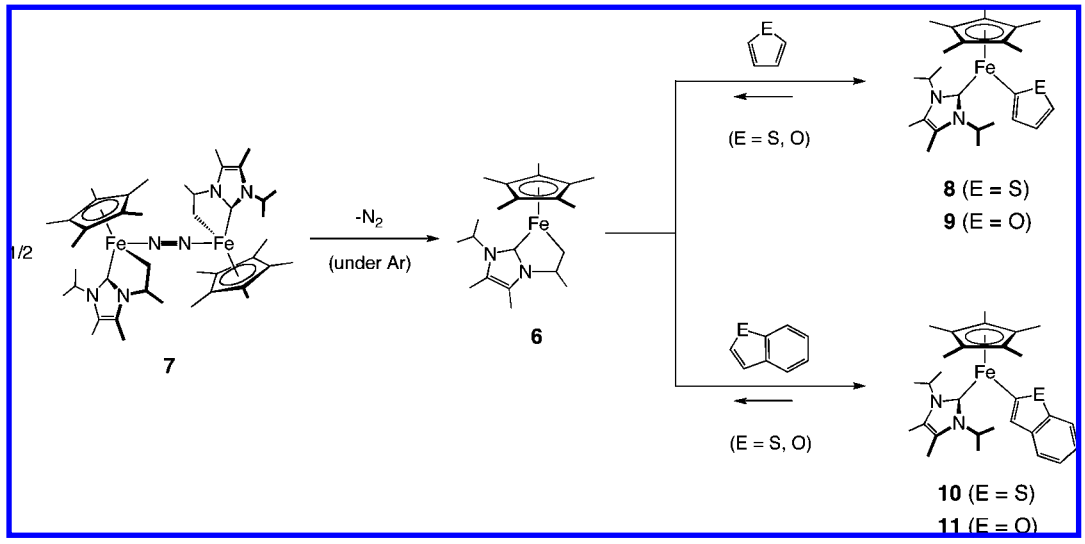

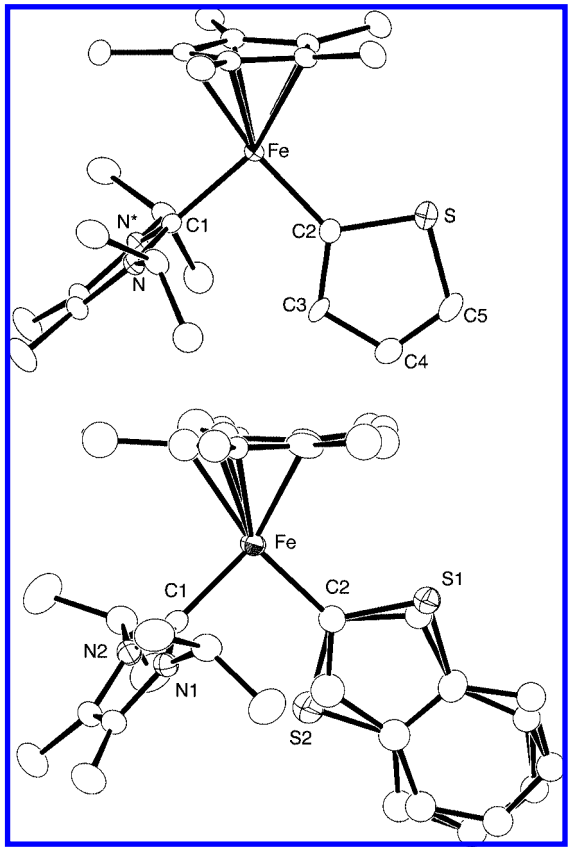

Figure 6. Molecular structures of **8** and **10** with thermal ellipsoids at the 50% probability level.

Table 1. Selected Bond Distances (Å) and Angles (deg) for Complexes **8**−**10**[a]

	8	9	10[b]
Fe−C(1)	1.959(2)	1.949(3)	1.956(2)
Fe−C(2)	1.962(2)	1.945(3)	1.971(2)
C(1)−N(1)	1.3679(17)	1.357(3)	1.366(3)
C(1)−N(2)	−	1.365(3)	1.356(4)
E−C(2)[c]	1.735(2)	1.413(4)	1.722(3),1.723(3)
E−C(5)[c]	1.710(2)	1.364(4)	1.706(3),1.614(3)
C(2)−C(3)	1.438(3)	1.380(4)	1.333(9),1.533(9)
C(3)−C(4)	1.442(3)	1.434(6)	1.475(8),1.514(8)
C(4)−C(5)	1.355(3)	1.303(7)	1.397(4)
C(1)−Fe−C(2)	91.93(9)	89.97(13)	92.50(10)
N(1)−C(1)−N(2)	103.89(15)	104.0(2)	104.6(2)
C(2)−E−C(5)[c]	95.18(12)	108.2(3)	93.20(18),95.47(18)
E−C(2)−C(3)[c]	107.41(15)	105.4(2)	105.6(4),108.0(3)
C(2)−C(3)−C(4)	112.7(2)	108.1(3)	123.1(6),109.6(6)
		Dihedral angles (deg)	
C(1)−Fe−C(2)/heteroaryl	0	0.20(14)	22.00(10),23.80(12)

[a] Labeling scheme as shown. [Fe] = Cp*Fe. [b] Distances and angles for both of the disordered 2-benzothienyl groups are listed. [c] E = S (**8** and **10**), O (**9**).

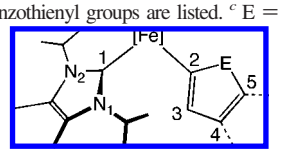

and L^{iPr} were observed in the ^1H NMR. The regio-selectivity of C−H bond cleavage demonstrated by the H/D scrambling is perplexing.

To further characterize the pyridyl complex, *tert*-butylisocyanide was added producing a diamagnetic adduct. Upon crystallization, only the 4-pyridyl complex Cp*Fe(L^{iPr})(CN^tBu)

Scheme 7

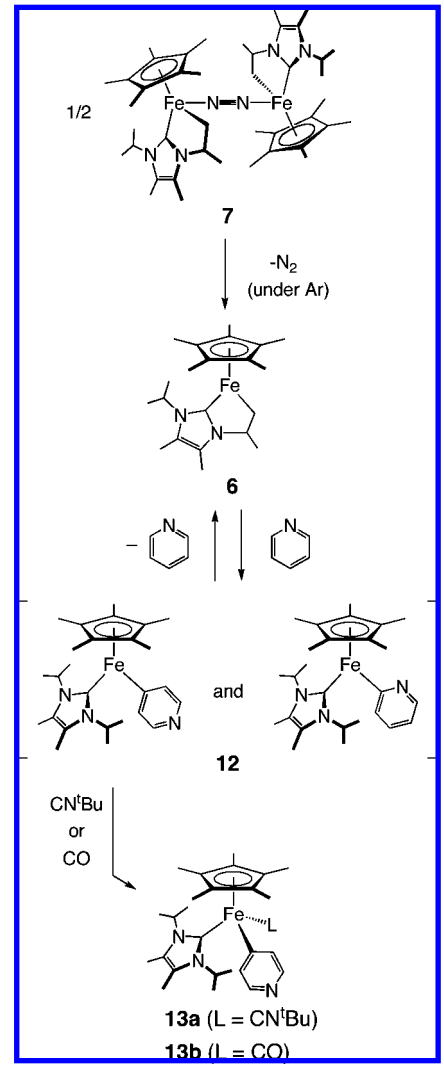

(4-C_5H_4N) (**13a**) was isolated in 41% yield. In a similar manner, the CO adduct of the 4-pyridyl complex Cp*Fe(L^{iPr})(CO)(4-C_5H_4N) (**13b**) was also crystallized in 26% yield. In accordance with C_1 symmetry, the L^{iPr} ligand exhibits six methyl signals in the ^1H NMR of **13a** and **13b**, while the signals for the 4-pyridyl group were found at δ 8.14 and 7.32 (**13a**) and at δ 8.18 and 7.37 (**13b**). The X-ray crystallographic analysis of **13a** also establishes C−H cleavage at the 4-position (see Supporting Information). The Fe−C(carbene) distance (1.9885(17) Å) is longer than those in the coordinatively unsaturated complexes

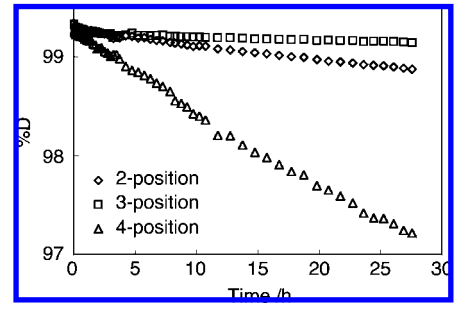

Figure 7. H/D scrambling between **6** and 200 equiv of pyridine-d_5 at room temperature: Time-dependent changes in deuterium ratios of the 2-, 3-, and 4-positions of pyridine-d_5 are plotted.

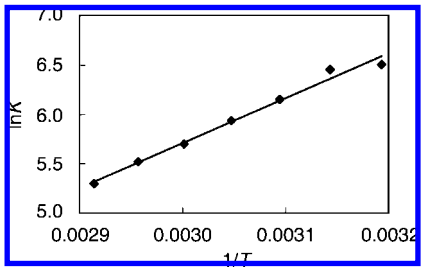

Figure 8. Van't Hoff plot for the equilibrium between **9** and **6** + furan. Thermodynamic data for the formation of **9** were determined as $\Delta H° = -9.0(5)$ kcal/mol and $\Delta S° = -16(1)$ eu.

8−**10**, consistent with the 18e iron center in **13a**. The Fe−C(pyridyl) distance (1.9971(16) Å) is comparable to those for iron-pyridyl and -quinolyl complexes (1.970(4)−2.004(8) Å).[21]

Equilibria of the C−H Bond Cleavage Reactions. In Scheme 6, reversibility of the C−H bond cleavage reactions is indicated. As noted above, the ^{1}H NMR spectra of these iron−heteroaryl complexes in C_6D_6 exhibit additional signals for **6**, and therefore it appears that complexes **8**−**11** are in equilibrium with **6** and the heteroarene. In order to determine the equilibrium constants for the reaction between **6** and furan, the concentrations of **6**, **9**, and furan were monitored by ^{1}H NMR spectroscopy. The ratio of the compounds reached a constant value within 1 h and remained unchanged over the next few hours. The equilibrium constant was estimated from the ratio of complexes **6** and **9** and free furan over the temperature range of 40−70 °C in C_6D_6, allowing the determination of the enthalpy and entropy from a Van't Hoff plot (Figure 8). The thermodynamic data for the formation of **8** were also determined in a similar manner. Whereas the signal intensities for **6** and the heteroarenes in the reactions with benzothiophene or benzofuran were too low to determine, the equilibrium constants for the reactions of **10** + thiophene or **11** + thiophene were successfully obtained. Thus these values and the equilibrium constant for the formation of **8** were used to calculate the thermodynamic data for the formation of **10** and **11** from **6**. As summarized in Chart 1, the values for $\Delta S°$ are negative in all cases, consistent with the addition of the heteroarenes to the iron complex. The negative entropy also indicates that the regeneration of **6** from iron-heteroaryl complexes becomes more favorable at elevated temperatures. The negative $\Delta H°$ values for **8**−**11** show that the sum of the strain energy of metallacycle and the bond energies for the Fe−C(sp^2) and C−H(sp^3) bonds in **8**−**11** is larger than the bond energies of the Fe−C(sp^3) bond in **6** and the C−H(sp^2) bond in the heteroarene. The data for complexes **8**−**11** also indicate that complexes derived from benzo-fused heteroarenes are thermodynamically preferred over those of thiophene and furan.

Mechanistic Aspects of the C−H Bond Cleavage of Thiophenes and Furans. The chemistry illustrated in Scheme 6 demonstrates that the C−H bond activation of thiophenes and furans occurs selectively at the 2-position. This C−H activation suggests that the reactions are initiated by interaction between the heteroarenes and the iron center. The heteroarenes are placed in such a way that the 2-position comes close to the methylene group of metallacycle. However, the heteroarenes adducts such as **A** in Scheme 8 have not been detected by ^{1}H NMR.

Whereas there are two possible pathways for the C−H bond cleavage step, namely oxidative addition and σ-bond metathesis, we assume that oxidative addition is less likely since the Fe(IV) state is uncommon for Cp*Fe complexes.[22,23] The alternative σ-bond metathesis is a nonredox process, and it can be described as a deprotonation of the C−H bond of the heteroarene promoted by the iron bound methylene group. The suggestion that the lithium atom of nBuLi interacts with the heteroatom of thiophenes or furans and the butyl group selectively deprotonates the 2-position to generate heteroaryl-lithium,[24,25] incorporates a similar pathway.

Coupling of Heteroarenes with Catecholborane. Development of new, selective methods to transform organic compounds via C−H bond cleavage is a major challenge in synthetic chemistry. Arylboron compounds are useful and important building blocks for Suzuki-Miyaura coupling reactions,[26] and thus the preparation of organoboron compounds via cleavage of C−H bonds is of significant value.[27] Since C−H activation of thiophenes or furans by **6** occurs selectively at the 2-position, we examined the borylation reactions.

The coupling reaction between thiophene and catecholborane (HBcat) was carried out by treatment of in situ generated **6** with

Chart 1

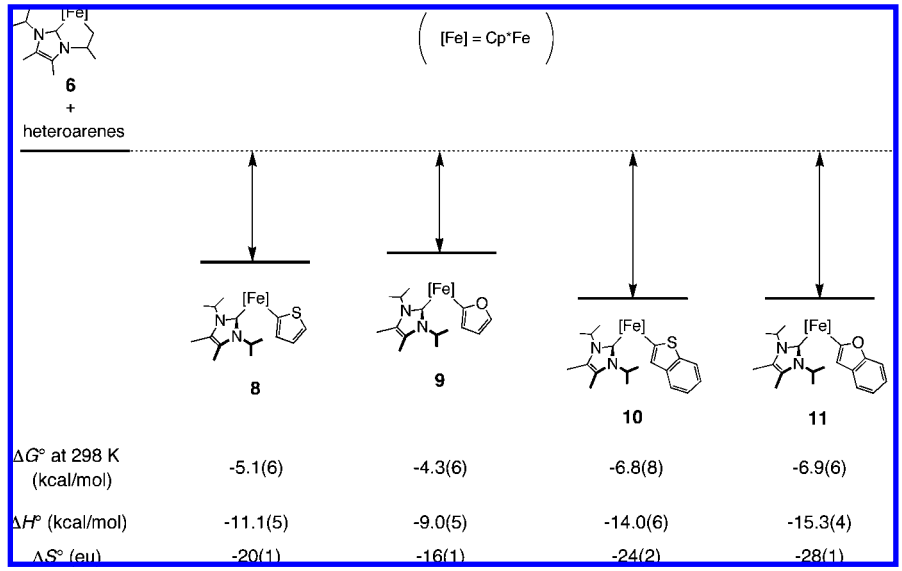

Scheme 8

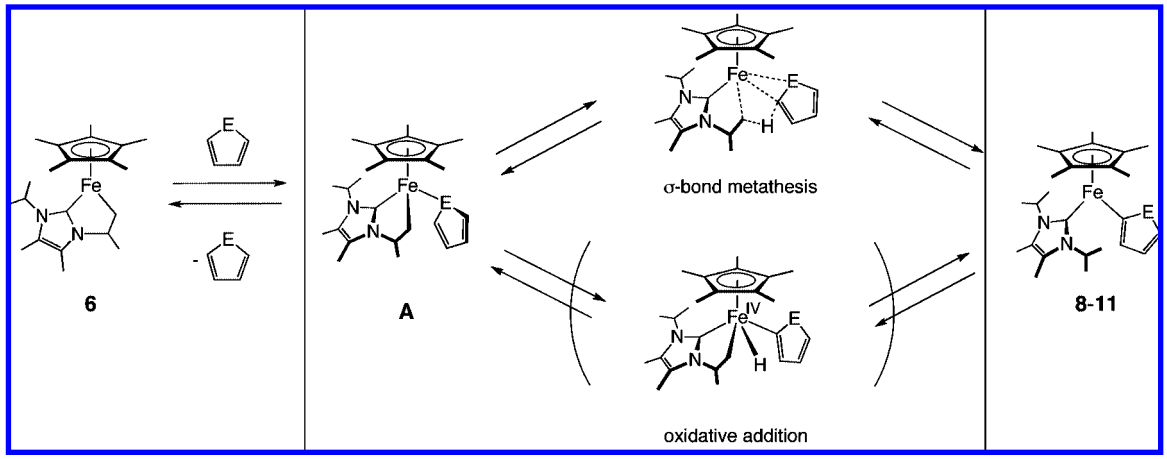

Scheme 9

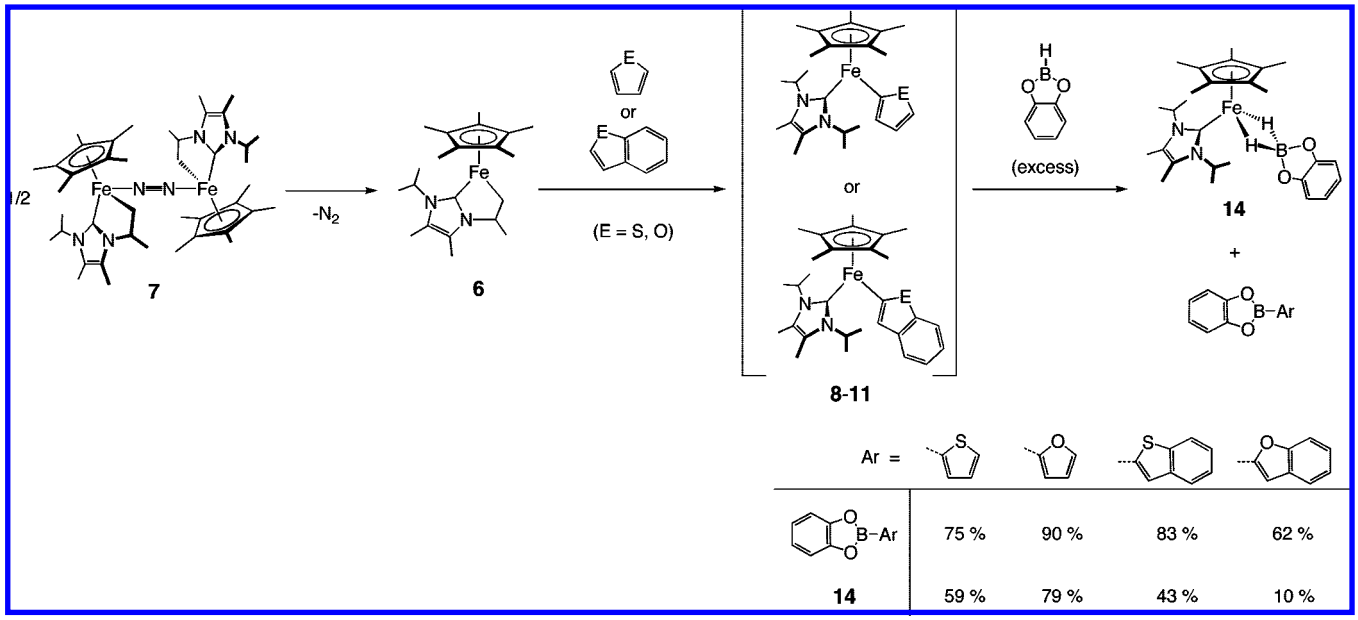

thiophene at room temperature, followed by addition of excess catecholborane (Scheme 9). In the ^{1}H NMR spectrum of the reaction mixture, new signals for a diamagnetic iron complex were observed together with a set of signals for 2-(catecholboryl)thiophene. The coupling of furan, benzothiophene, or benzofuran with HBcat proceeded similarly, giving rise to the same iron complex and the 2-boryl-heteroarenes. The new iron complex was identified as Cp*Fe(L^{iPr})(H$_2$Bcat) (**14**), whose structure was confirmed by a single crystal X-ray analysis as shown in Figure 9. The Fe−C(1) distance (1.973(3) Å) is slightly longer than those for the unsaturated complexes **2b** and **8**−**10** (1.949(3)−1.959(2) Å). The [H$_2$Bcat]$^-$ ligand is attached to the iron center with two Fe−H−B bonds, and the Fe−B distance of 2.002(3) Å is in the range of known Fe−H−B complexes (1.855(2)−2.304(21) Å).[28] In the ^{1}H NMR, the Fe−*H*−B hydride was observed as a broad signal at δ −15.6 (2H, $w_{1/2}$ = 205 Hz).

A proposed reaction mechanism is shown in Scheme 10. Reactions between **6** and heteroarenes yield the iron-heteroaryl complexes **8**-**11**, and the following borylation process probably provides the iron-hydride intermediate [Cp*Fe(L^{iPr})H], which

(21) (a) le Borgue, G.; Grandjean, D. *J. Organomet. Chem.* **1975**, *92*, 381–392. (b) Hunter, A. D.; Chukwu, R.; Santarsiero, B. D.; Bott, S. G.; Atwood, J. L. *J. Organomet. Chem.* **1996**, *526*, 1–14. (c) Chukwu, R.; Hunter, A. D.; Santarsiero, B. D.; Bott, S. G.; Atwood, J. L. *Organometallics* **1992**, *11*, 589–597.

(22) In the case of iron hydrides, the formal Fe(IV) oxidation state can only be found in some silyl complexes[22] and cationic dihydride/diphosphine complexes.[23] For silyl complexes, see: (a) Manojlovic-Muir, L.; Muir, K. W.; Ibers, J. A. *Inorg. Chem.* **1970**, *9*, 447–452. (b) Asirvatham, V. S.; Yao, Z.; Klabunde, K. J. *J. Am. Chem. Soc.* **1994**, *116*, 5493–5494. (c) Yao, Z.; Klabunde, K. J. *Organometallics* **1995**, *14*, 5013–5014. (d) Yao, Z.; Klabunde, K. J.; Asirvatham, A. S. *Inorg. Chem.* **1995**, *34*, 5289–5294. (e) Yao, Z.; Klabunde, K. J.; Hupton, A. C. *Inorg. Chim. Acta* **1997**, *259*, 119–124.

(23) For cationic dihydride/diphosphine complexes of Fe(IV), see: (a) Jiménez-Tenorio, M.; Puerta, M. C.; Valerga, P. *Organometallics* **1994**, *13*, 3330–3337. (b) Hamon, J.-R.; Hamon, P.; Toupet, L.; Costuas, K.; Saillard, J.-Y. *C. R. Chimie* **2002**, *5*, 89–98.

(24) See for example: (a) Gilman, H.; Shirley, D. A. *J. Am. Chem. Soc.* **1949**, *71*, 1870–1871. (b) Shirley, D. A.; Cameron, M. D. *J. Am. Chem. Soc.* **1950**, *72*, 2788–2789.

(25) See for example: (a) Benkeser, R. A.; Currie, R. B. *J. Am. Chem. Soc.* **1948**, *70*, 1780–1782. (b) DiMenna, W. S. *Tetrahedron Lett.* **1980**, *21*, 2129–2132.

(26) (a) Miyaura, N.; Suzuki, A. *Chem. Rev.* **1995**, *95*, 2457–2483. (b) Suzuki, A. *J. Organomet. Chem.* **1999**, *576*, 147–168.

(27) Ishiyama, T.; Miyaura, N. *Chem. Rec.* **2004**, *3*, 271–280.

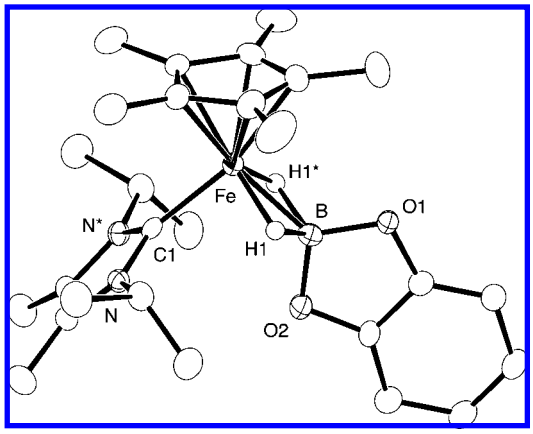

Figure 9. Molecular structure of **14** with thermal ellipsoids at the 50% probability level. Selected bond distances (Å) and angles (°): Fe−B = 2.002(3), Fe−C(1) = 1.973(3), Fe−H(1) = 1.58(2), B−H(1) = 1.38(2), C(1)−N(1) = 1.366(2), B−Fe−C(1) = 94.19(14), O(1)−B−O(2) = 106.7(2), B−Fe−H(1) = 43.3(10), Fe−B−H = 52.0(12), N−C(1)−N* = 103.7(2).

Scheme 10. Possible Reaction Pathway ([Fe] = Cp*Fe)

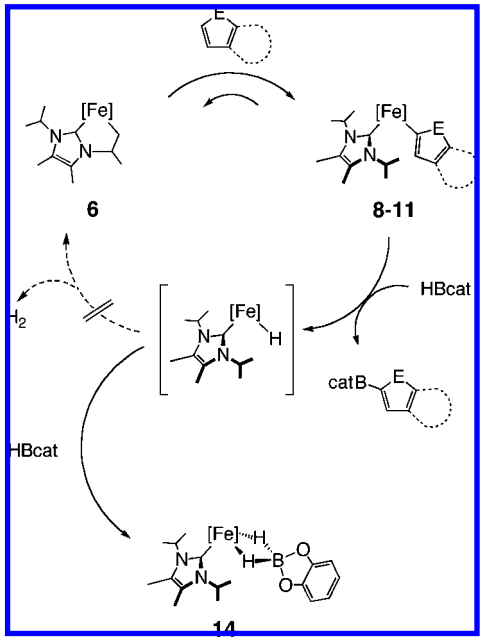

is trapped by HBcat to form the borohydride complex **14**. With reference to the formation of **6** via cyclometalation (Scheme 3), one might expect a similar cyclometalation from [Cp*Fe(L^{iPr})H] to regenerate **6**, completing the formal catalytic cycle for dehydrogenative coupling of heteroarenes and HBcat. However, attempts to achieve a catalytic reaction have been unsuccessful because of the inevitable formation of complex **14**, which is thermally stable and unreactive toward heteroarenes or HBcat. In the coupling of thiophene with HBcat, the yields of **14** and 2-(catecholboryl)thiophene were 59% and 75%, respectively, by ^{1}H NMR based on the C_6Me_6 internal standard.

Conclusions

Intramolecular C−H bond cleavage reactions of N-heterocyclic carbene ligands (L^R) have been used to synthesize coordinatively unsaturated metallacycle Cp*Fe complexes. The formation of the metallacyle is faster for L^{iPr} than for L^{Mes}, due to the more favorable location of the methyl group. The coordinative unsaturation of the iron center in the metallacyclic complex **6** enables reversible binding of N_2 to produce a dinuclear end-on N_2 complex **7**. Complex **6** also carries out reversible C−H bond activation of the 2-positions of thiophenes and furans at ambient conditions to produce the iron-heteroaryl complexes **8**−**11**. A key for the selective C−H bond activation of thiophenes and furans is the close proximity of the 2-position to the Fe-methylene group when the heteroarenes approach the iron center. The driving force for C−H bond activation may be provided by the ring opening, generating new C−H(^{i}Pr) and Fe−C(aryl) bonds and releasing the ring strain of the metallacycle. The heteroaryl groups in complexes **8**−**11** were found to give 2-boryl-heteroarenes upon treatment with catecholborane.

Experimental Section

General Procedures. All reactions were carried out using standard Schlenk techniques and a glovebox under a nitrogen or argon atmosphere. Toluene, ether, THF, pentane, and hexane were purified by the method of Grubbs,[29] where the solvents were passed over columns of activated alumina and a supported copper catalyst supplied by Hansen & Co. Ltd. Solvents, degassed and distilled from sodium benzophenone ketyl were also used. Deuterated solvents, C_6D_6 and pyridine-d_5, were vacuum-transferred from sodium or CaH_2 prior to use. ^{1}H and ^{13}C{^{1}H} NMR spectra were acquired on a JEOL ECA-600. ^{1}H NMR signals were referenced to the residual proton peak of the deuterated solvent. The ^{11}B chemical shift was referenced to external $(Me_3N)BH_3$ in C_6D_6 (−9.1 ppm). The ^{13}C chemical shifts were relative to the carbon signals for the deuterated solvents. Infrared spectra were recorded on a JASCO A3 spectrometer. Raman spectra were recorded on a Perkin-Elmer 2000 NIR FT-Raman spectrometer. Elemental analyses were performed on a LECO-CHNS-932 elemental analyzer where the crystalline samples were sealed in silver capsules under nitrogen. X-ray diffraction data were collected on a Rigaku AFC8 or a Rigaku RA-Micro7 equipped with a CCD area detector using graphite-monochromatized Mo Kα radiation. Cp*Fe{$N(SiMe_3)_2$} (**1**)[8] and N-heterocyclic carbenes[13] were prepared according to literature procedures.

Synthesis of Cp*Fe(L^{Mes})Cl (2a). To a toluene (60 mL) solution of Cp*Fe{$N(SiMe_3)_2$} (**1**) (430 mg, 1.22 mmol) was added a toluene suspension of the imidazolium salt (HL^{Mes})(Cl) (417 mg, 1.22 mmol) at −78 °C. The reaction mixture was allowed to warm to room temperature with stirring for 3 h. The solvent was removed under reduced pressure, and the resulting solid was extracted with Et_2O (40 mL) and centrifuged. The solution was concentrated to *ca.* 20 mL, and cooled at −35 °C to give Cp*Fe(L^{Mes})Cl (**2a**, 598 mg, 92% yield) as brownish green crystals. Single crystals for X-ray analysis were obtained from toluene. ^{1}H NMR (C_6D_6): δ 169 (15H, Cp*), 76.0 (6H, Mes), 39.1 (2H, $C(NMes)_2C_2H_2$), −11.4 (6H, Mes), −5 to −23 (very broad, 4H, Mes), −43.6 (6H, Mes). Anal. Calcd for $C_{31}H_{39}N_2ClFe$: C, 70.13; H, 7.40; N, 5.28. Found: C, 70.12; H, 7.04; N, 5.33.

Synthesis of Cp*Fe(L^{iPr})Cl (2b). To a toluene (100 mL) solution of Cp*Fe{$N(SiMe_3)_2$} (**1**) (805 mg, 2.29 mmol) was added a toluene suspension of the imidazolium salt (HL^{iPr})(Cl) (496 mg, 2.29 mmol) at −78 °C. The reaction mixture was allowed to warm to room

(28) (a) Ghilardi, C. A.; Innocenti, P.; Midollini, S.; Orlandini, A. *J. Chem. Soc., Dalton Trans.* **1985**, 605–609. (b) Nlate, S.; Guènot, P.; Sinbandhit, S.; Toupet, L.; Lapinte, C.; Guerchais, V. *Angew. Chem., Int. Ed. Engl.* **1994**, *33*, 2218–2219. (c) Hillier, A. C.; Jacobsen, H.; Gusev, D.; Schmalle, H. W.; Berke, H. *Inorg. Chem.* **2001**, *40*, 6334–6337. (d) Guilera, G.; McGrady, G. S.; Steed, J. W.; Kaltsoyannis, N. *New J. Chem.* **2004**, *28*, 444–446. (e) Koutmos, M.; Georgakaki, I. P.; Coucouvanis, D. *Inorg. Chem.* **2006**, *45*, 3648–3656. (f) Mehn, M. P.; Brown, S. D.; Paine, T. K.; Brennessel, W. W.; Cramer, C. J.; Peters, J. C.; Que, L., Jr. *Dalton Trans.* **2006**, 1347–1351.
(29) Pangborn, A. B.; Giardello, M. A.; Grubbs, R. H.; Rosen, R. K.; Timmers, F. J. *Organometallics* **1996**, *15*, 1518–1520.

temperature with stirring for 3 h. The solvent was removed under reduced pressure, and the resulting solid was extracted with Et_2O (50 mL) and centrifuged. The solution was concentrated to *ca.* 30 mL, and cooled at −35 °C to give Cp*Fe(L^{iPr})Cl (**2b**) (638 mg, 69% yield) as dark green crystals. ^{1}H NMR (C_6D_6): δ 120 (15H, Cp*), 19.8 (6H, C(N^{i}Pr)$_2$C$_2$*Me*$_2$), 11.5 (6H, ^{i}Pr), −9.2 (6H, ^{i}Pr), −12.5 (2H, ^{i}Pr). Anal. Calcd for $C_{21}H_{35}N_2ClFe$: C, 62.00; H, 8.67; N, 6.89. Found: C, 61.62; H, 8.20; N, 7.03.

Synthesis of Cp*Fe(L^{Mes})Me (3a). To an Et_2O (30 mL) solution of **2a** (243 mg, 0.458 mmol) was added 0.54 mL of methyllithium (0.93 M in Et_2O, 0.50 mmol) at −78 °C. The reaction mixture was allowed to warm to room temperature with stirring for 1 h. The solvent was removed under reduced pressure, and the resulting solid was extracted with hexane (10 mL) and centrifuged. The solution was concentrated to *ca.* 3 mL, and cooled at −30 °C to give Cp*Fe(L^{Mes})Me (**3a**) (197 mg, 84% yield) as orange crystals. ^{1}H NMR (C_6D_6): δ 38.9 (15H, Cp*), 34.8 (2H, C(NMes)$_2$C$_2$*H*$_2$), 32.3 (6H, Mes), −1.9 (2H, Mes), −3.9 (6H, Mes), −8.9 (2H, Mes), −30.4 (6H, Mes), −458 (3H, Fe-Me). Anal. Calcd for $C_{21}H_{35}N_2ClFe$: C, 75.28; H, 8.29; N, 5.49. Found: C, 75.10; H, 8.63; N, 5.67.

Synthesis of Cp*Fe(L^{Mes})Ph (3b). To an Et_2O (20 mL) solution of **2a** (92 mg, 0.017 mmol) was added 90 μL of phenyllithium (1.9 M in Bu_2O, 0.017 mmol) at −78 °C. The reaction mixture was allowed to warm to room temperature with stirring for 3 h. The solvent was removed under reduced pressure, and the resulting solid was extracted with hexane (7 mL) and centrifuged. The solution was concentrated to *ca.* 1 mL, and cooled at −30 °C to give Cp*Fe(L^{Mes})Ph (**3b**) (76 mg, 77% yield) as orange crystals. ^{1}H NMR (C_6D_6): δ 45.1 (15H, Cp*), 28.5 (6H, Mes), 23.2 (2H, C(NMes)$_2$C$_2$*H*$_2$), 13.7 (1H, Ph), 3.2 (2H, Mes), −0.7 (6H, Mes), −5.1 (2H, Mes), −8.9(2H, Mes), −28.6 (6H, Mes), −36 (br, 2H, Ph). Anal. Calcd for $C_{37}H_{44}N_2Fe$: C, 77.61; H, 7.75; N, 4.89. Found: C, 77.77; H, 8.20; N, 5.06.

Synthesis of Cp*Fe{κ^2-(C,C)-L′^{Mes}} (4). A toluene (10 mL) solution of **3a** (97 mg, 0.19 mmol) was stirred at 60 °C for 3 days. The solvent was removed under reduced pressure, and the resulting solid was extracted with hexane (7 mL) and centrifuged. The solution was concentrated to *ca.* 1 mL, and cooled at −30 °C to give Cp*Fe{κ^2-(C,C)-L′^{Mes}} (**4**) (72 mg, 81% yield) as dark green crystals. ^{1}H NMR (C_6D_6): δ 48.6 (15H, Cp*), 45.3 (1H, C(NMes)$_2$C$_2$*H*$_2$), 14.8 (1H, C(NMes)$_2$C$_2$*H*$_2$), −0.2 (Mes), −1.7 (3H, Mes), −8.4 (1H, Mes), −8.7 (3H, Mes), −11.9 (3H, Mes), −12.8 (3H, Mes′), −14.6 (3H, Mes′), −30.6 (1H, Mes′), −42.4 (1H, Mes′). Anal. Calcd for $C_{31}H_{38}N_2Fe$: C, 75.30; H, 7.75; N, 5.67. Found: C, 75.35; H, 7.86; N, 5.64.

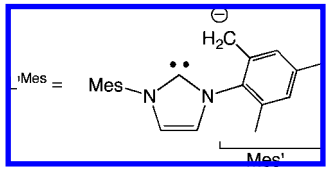

Kinetic Study of the Thermolysis of 3a. To a C_6D_6 (3.8 mL) solution of **3a** (55 mg, 0.11 mmol) was added 9 mg of hexamethylbenzene as an internal standard. Portions of this solution were charged into five NMR tubes, and the tubes were capped with a J-Young valve. The methyl signals of **3a** (δ −3.9 and −30.4 at 25 °C) were monitored by ^{1}H NMR at 40∼80 °C and were integrated at intervals. Rate constants k were determined to be 1.98×10^{-6} (40 °C), 5.14×10^{-6} (50 °C), 1.85×10^{-5} (60 °C), 4.17×10^{-5} (70 °C), and 1.32×10^{-4} (80 °C). An Eyring plot (Figure 3) yielded the activation parameters $\Delta H^{\ddagger}$ = 22.4(9) kcal/mol and $\Delta S^{\ddagger}$ = −13(3) eu.

Synthesis of Cp*Fe{κ^2-(C,C)-L′^{Mes}}(CO) (5). A toluene (10 mL) solution of **4** (72 mg, 0.15 mmol) was stirred for 20 min under 1 atm of CO at room temperature. The solvent was removed under reduced pressure, and the resulting solid was extracted with hexane (8 mL) and centrifuged. The solution was concentrated to *ca.* 3 mL, and cooled at 0 °C to give Cp*Fe{κ^2-(C,C)-L′^{Mes}}(CO) (**5**) (40 mg, 53% yield) as orange crystals. ^{1}H NMR (C_6D_6): δ 7.13 (s, 1H, Mes′), 6.96 (s, 1H, Mes′), 6.84 (s, 1H, Mes), 6.83 (d, J = 2.0 Hz, 1H, C(NMes)$_2$C$_2$*H*$_2$), 6.61 (s, 1H, Mes), 6.08 (d, J = 2.0 Hz, 1H, C(NMes)$_2$C$_2$*H*$_2$), 2.22 (s, 3H, Mes), 2.15 (s, 6H, Mes), 2.09 (s, 3H, Mes′), 2.08 (s(br), 1H, Fe-C*H*$_2$), 2.072 (s, 3H, Mes′), 2.065 (s(br), 1H, Fe−C*H*$_2$), 1.39 (s, 15H, Cp*). ^{13}C{^{1}H} NMR (C_6D_6): δ 226.1 (CO), 209.4 (*C*(NMes)$_2$C$_2$H$_2$), 151.9 (Mes), 139.5 (Mes), 138.9 (Mes), 138.4 (Mes), 138.1 (Mes), 135.3 (Mes′), 134.9 (Mes′), 130.3 (Mes′), 128.0 (Mes′), 126.7 (Mes′), 126.2 (Mes′), 123.3 (C(NMes)$_2$*C*$_2$H$_2$), 123.1 (C(NMes)$_2$*C*$_2$H$_2$), 90.4 (*C*$_5$Me$_5$), 21.6 (Mes), 20.1 (Mes), 19.7 (Mes′), 19.5 (Mes′), 10.1 (C$_5$*Me*$_5$), 8.9 (Fe-*C*H$_2$). IR (KBr, cm^{-1}): 1872 (s, CO). Anal. Calcd for $C_{32}H_{38}N_2OFe$: C, 73.56; H, 7.33; N, 5.36. Found: C, 73.09; H, 7.39; N, 5.40.

Synthesis of Cp*Fe{κ^2-(C,C)-L′^{iPr}} (6). To a Et_2O (30 mL) solution of **2b** (67 mg, 0.15 mmol) was added 0.15 mL of methyllithium (1.0 M in Et_2O, 0.15 mmol) at −78 °C under an argon atmosphere. The reaction mixture was allowed to warm to room temperature and stirred for 3 h. The solvent was removed under reduced pressure, and the resulting solid was extracted with hexane (10 mL) and centrifuged. The solution was concentrated to *ca.* 1 mL, and cooled at −30 °C to give Cp*Fe{κ^2-(C,C)-L′^{iPr}} (**6**) (60 mg, 98% yield) as yellowish-brown crystals. ^{1}H NMR (C_6D_6): δ 45.5 (15H, Cp*), 44.4 (3H, C(N^{i}Pr)$_2$C$_2$*Me*$_2$), 37.6 (3H, C(N^{i}Pr)$_2$C$_2$*Me*$_2$), 2.0 (3H, ^{i}Pr), −17.6 (3H, ^{i}Pr), −22.9 (3H, ^{i}Pr), −36.9 (1H, ^{i}Pr), −83.4 (1H, ^{i}Pr). Anal. Calcd for $C_{21}H_{34}N_2Fe$: C, 68.10; H, 9.25; N, 7.56. Found: C, 67.87; H, 8.98; N, 7.80.

Formation of [Cp*Fe{κ^2-(C,C)-L′^{iPr}}]$_2$(μ-η^1:η^1-N$_2$) (7). A hexane (5 mL) solution of **6** (58 mg, 0.18 mmol) was kept standing under an N_2 atmosphere at room temperature. After 1 h, red crystals of [Cp*Fe{κ^2-(C,C)-L′^{iPr}}]$_2$(μ-η^1:η^1-N$_2$) (**7**) grew in 92% yield (80 mg). The ^{1}H NMR spectrum exhibited broad signals for **6** together with a sharp singlet at δ 1.66, which is assignable to Cp* of **7**. Raman (cm^{-1}): 2126 (w, N≡N). Anal. Calcd for $C_{42}H_{68}N_6Fe_2$: C, 65.62; H, 8.92; N, 10.93. Found: C, 64.14; H, 8.66; N, 9.58. We have been unable to obtain a satisfactory elemental analysis. Single crystals of diffraction quality always gave low values for carbon and nitrogen. We believe that the compound is analytically pure, but either its thermal lability or incomplete combustion is responsible for the unsatisfactory analysis.

Synthesis of Cp*Fe(L^{iPr})(2-C_4H_3S) (8). A yellowish-brown solution of **6** (0.15 mmol) was prepared by dissolving red crystals of **7** (58 mg) in hexane (5 mL) under an argon atmosphere. To this solution was added thiophene (24 μL, 0.30 mmol) at room temperature. After stirring for 2 h, the reaction mixture was centrifuged. The solution was concentrated to *ca.* 2 mL, and cooled at 0 °C to give Cp*Fe(L^{iPr})(2-C_4H_3S) (**8**, 52 mg, 76%) as brownish green crystals. ^{1}H NMR (C_6D_6): δ 42.6 (15H, Cp*), 20.4 (1H, C_4H_3S), 19.7 (6H, L^{iPr}), 7.6 (6H, L^{iPr}), 3.0 (6H, L^{iPr}), −23.9 (1H, C_4H_3S), −58 (1H, C_4H_3S), −174 (2H, ^{i}Pr). Anal. Calcd for $C_{25}H_{38}N_2SFe$: C, 66.07; H, 8.43; N, 6.16; S, 7.06. Found: C, 65.70; H, 8.14; N, 6.38; S, 7.02.

Synthesis of Cp*Fe(L^{iPr})(2-C_4H_3O) (9). A solution of **6** (0.15 mmol) was prepared by dissolving red crystals of **7** (56 mg) in pentane (5 mL) under an argon atmosphere. To this solution was added furan (11 μL, 0.15 mmol) at room temperature. After stirring for 2 h, the reaction mixture was centrifuged. The solution was concentrated to *ca.* 1 mL, and cooled at 0 °C to give Cp*Fe(L^{iPr})(2-C_4H_3O) (**9**, 46 mg, 72%) as brownish green crystals. ^{1}H NMR (C_6D_6): δ 44.3 (15H, Cp*), 32.2 (1H, C_4H_3O), 18.4 (6H, L^{iPr}), 6.8 (6H, L^{iPr}), 5.2 (6H, L^{iPr}), −77.9 (1H, C_4H_3O), −82 (1H, C_4H_3O), −173 (2H, ^{i}Pr). Anal. Calcd for $C_{25}H_{38}N_2OFe$: C, 68.49; H, 8.74; N, 6.39 Found: C, 68.10; H, 8.31; N, 6.59.

Synthesis of Cp*Fe(L^{iPr})(2-C_8H_5S) (10). A solution of **6** (0.14 mmol) was prepared by dissolving red crystals of **7** (54 mg) in toluene (5 mL) under an argon atmosphere. To this solution was added benzothiophene (19 mg, 0.14 mmol) at room temperature. After stirring for 2 h, the reaction mixture was centrifuged. The

solution was concentrated to *ca.* 1 mL, and cooled at 0 °C to give Cp*Fe(L^{iPr})(2-C_8H_5S) (**10**, 42 mg, 59%) as brownish green crystals. ^{1}H NMR (C_6D_6): δ 46.0 (15H, Cp*), 22.3 (1H, C_8H_5S), 21.6 (6H, L^{iPr}), 13.3 (1H, C_8H_5S), 7.6 (6H, L^{iPr}), 4.0 (6H, L^{iPr}), 0.5 (1H, C_8H_5S), −0.1 (1H, C_8H_5S), −58 (1H, C_8H_5S), −170 (2H, ^{i}Pr). Anal. Calcd for $C_{29}H_{40}N_2SFe$: C, 69.03; H, 7.99; N, 5.55; S, 6.36. Found: C, 68.91; H, 7.72; N, 5.69; S, 5.93.

Synthesis of Cp*Fe(L^{iPr})(2-C_8H_5O) (11). A solution of **6** (0.21 mmol) was prepared by dissolving red crystals of **7** (82 mg) in toluene (10 mL) under an argon atmosphere. To this solution was added benzofuran (26 μL, 0.24 mmol) at room temperature. After stirring for 2 h, the reaction mixture was centrifuged. The solution was concentrated to *ca.* 1 mL, and cooled at 0 °C to give Cp*Fe(L^{iPr})(2-C_8H_5O) (**11**, 68 mg, 65%) as brownish green crystals. ^{1}H NMR (C_6D_6): δ 48.6 (15H, Cp*), 20.2 (1H, C_8H_5O), 19.0 (6H, L^{iPr}), 16.0 (1H, C_8H_5O), 8.5 (6H, L^{iPr}), 7.2 (6H, L^{iPr}), −9.1 (1H, C_8H_5O), −16.9 (1H, C_8H_5O), −64.0 (1H, C_8H_5O), −161 (2H, ^{i}Pr). Anal. Calcd for $C_{29}H_{40}N_2OFe$: C, 71.30; H, 8.25; N, 5.74. Found: C, 71.38; H, 7.76; N, 5.74.

Reaction of 6 with Pyridine. A solution of **6** (0.018 mmol) was prepared by dissolving red crystals of **7** (7 mg) in C_6D_6 (0.6 mL) under an argon atmosphere. To this solution was added pyridine (15 μL, 0.19 mmol) at room temperature. The reaction mixture was monitored by ^{1}H NMR, and the dominant formation of the pyridyl complex Cp*Fe(L^{iPr})(C_5H_4N) (**12**) was observed. ^{1}H NMR (C_6D_6): δ 47.7 (15H, Cp*), 23.4 (6H, L^{iPr}), 4.9 (6H, L^{iPr}), 2.8 (6H, L^{iPr}), −186 (2H, ^{i}Pr). The proton signals appearing at δ 22.5, 19.7, and 5.4 may be ascribed to the pyridyl group.

Synthesis of Cp*Fe(L^{iPr})(CN^{t}Bu)(4-C_5H_4N) (13a). A solution of **6** (0.16 mmol) was prepared by dissolving red crystals of **7** (60 mg) in pyridine (4 mL) under an argon atmosphere. After stirring for 1 h at room temperature, *tert*-butylisocyanide (20 μL, 0.18 mmol) was added at −40 °C. The reaction mixture was allowed to warm to room temperature with stirring for 2 h. The solvent was removed under reduced pressure, and the resulting solid was extracted with a 2:1 (v/v) mixture of hexane/Et_2O (15 mL) and centrifuged. The solution was concentrated to *ca.* 5 mL, and cooled at 0 °C to give Cp*Fe(L^{iPr})(CN^{t}Bu)(4-C_5H_4N) (**13a**, 34 mg, 41% yield) as orange crystals. ^{1}H NMR (C_6D_6): δ 8.14 (d, J = 4.8 Hz, 2H, 2-Py), 7.32 (d, J = 4.8 Hz, 2H, 3-Py), 6.09 (sept, J = 6.7 Hz, 1H, ^{i}Pr), 5.23 (sept, J = 6.7 Hz, 1H, ^{i}Pr), 1.76 (s, 3H, $CN_2C_2Me_2$), 1.65 (s, 3H, $CN_2C_2Me_2$), 1.64 (s, 15H, Cp*), 1.59 (d, J = 6.7 Hz, 3H, ^{i}Pr), 1.26 (d, J = 6.7 Hz, 3H, ^{i}Pr), 1.16 (d, J = 6.7 Hz, 3H, ^{i}Pr), 1.09 (s, 9H, CN^{t}Bu), 0.51 (d, J = 6.7 Hz, 3H, ^{i}Pr). ^{13}C{^{1}H} NMR (C_6D_6): δ 206.3 (*C*N^{t}Bu), 199.8, 197.0 (N*C*N, 4-Py), 144.3 (2-, 3-Py), 127.5, 126.1 ($CN_2C_2Me_2$), 89.7 (C_5Me_5), 56.8 (CN^t*Bu*), 52.4, 52.3 (^{i}Pr), 32.2 (CN^{t}Bu), 24.9 (^{i}Pr), 24.4 (^{i}Pr), 24.2 (^{i}Pr), 21.6 (^{i}Pr), 11.3 (C_5Me_5). IR (KBr, pellet): 1897 (s, C≡N) cm^{-1}. Anal. Calcd for $C_{31}H_{48}N_4Fe$: C, 69.91; H, 9.08; N, 10.52. Found: C, 70.06; H, 8.90; N, 10.25.

Synthesis of Cp*Fe(L^{iPr})(CO)(4-C_5H_4N) (13b). A solution of **6** (0.18 mmol) was prepared by dissolving red crystals of **7** (64 mg) in pyridine (4 mL) under an argon atmosphere. After stirring for 1 h, the flask was charged with 1 atm CO at −40 °C. The reaction mixture was allowed to warm to room temperature and stirred for 2 h. The solvent was removed under reduced pressure, and the resulting solid was extracted with Et_2O (10 mL) and centrifuged. The solution was concentrated to *ca.* 2 mL, and cooled at 0 °C to give Cp*Fe(L^{iPr})(CO)(4-C_5H_4N) (**13b**, 21 mg, 26% yield) as orange crystals. ^{1}H NMR (C_6D_6): δ 8.18 (d, J = 4.6 Hz, 2H, 2-Py), 7.37 (d, J = 4.6 Hz, 2H, 3-Py), 5.95 (brs, 1H, ^{i}Pr), 5.04 (brs, 1H, ^{i}Pr), 1.64 (s, 3H, $CN_2C_2Me_2$), 1.58∼1.51 (m, 21H, Cp*, $CN_2C_2Me_2$ and ^{i}Pr), 1.18 (brs, 3H, ^{i}Pr), 1.08 (brs, 3H, ^{i}Pr), 0.36 (brs, 3H, ^{i}Pr). ^{13}C{^{1}H} NMR (C_6D_6): δ 226.9 (CO), 193.1, 189.5 (4-Py, $CN_2C_2Me_2$), 145.3, 143.6 (2-, 3-Py), 127.8 ($CN_2C_2Me_2$), 126.8 ($CN_2C_2Me_2$), 91.8 (C_5Me_5), 52.9 (^{i}Pr), 52.4 (^{i}Pr), 24.0 (^{i}Pr), 23.8 (^{i}Pr), 23.6 (^{i}Pr), 21.3 (^{i}Pr), 10.8 (C_5Me_5). IR (KBr, cm^{-1}): 1889 (s, CO). Anal. Calcd for $C_{27}H_{39}N_3OFe$: C, 67.92; H, 8.23; N, 8.80. Found: C, 68.19; H, 7.82; N, 8.78.

Table 2. Crystal Data for Cp*Fe(L^{Mes})Cl (**2a**), Cp*Fe(L^{iPr})Cl (**2b**), Cp*Fe(L^{Mes})Me (**3a**), Cp*Fe(L^{Mes})Ph (**3b**), Cp*Fe{κ^2-(C,C)-L^{Mes}}(CO) (**5**), Cp*Fe{κ^2-(C,C)-L^{iPr}} (**6**), [Cp*Fe{κ^2-(C,C)-L^{iPr}}]$_2$(μ-η^1:η^1-N_2) (**7**), Cp*Fe(L^{iPr})(2-C_4H_3O) (**8**), Cp*Fe(L^{iPr})(2-C_4H_3S) (**9**•1/2C_5H_{12}), Cp*Fe(L^{iPr})(2-C_8H_5S) (**10**), Cp*Fe(L^{iPr})(CN*t*Bu)(4-C_5H_4N) (**13a**), and Cp*Fe(L^{iPr})(H_2Bcat) (**14**)

	2a·C_7H_8	**2b**	**3a**	**3b**	**5**	**6**	**7**	**8**	**9**·1/2C_5H_{12}	**10**	**13a**	**14**
formula	$C_{38}H_{47}ClN_2Fe$	$C_{31}H_{51}N_2ClFe$	$C_{32}H_{42}N_2Fe$	$C_{37}H_{44}N_2Fe$	$C_{32}H_{38}N_2OFe$	$C_{32}H_{52}N_2Fe$	$C_{32}H_{52}N_4Fe$	$C_{25}H_{38}N_2SFe$	$C_{27.5}H_{44}N_2OFe$	$C_{32}H_{52}N_2SFe$	$C_{31}H_{48}N_4Fe$	$C_{27}H_{41}BN_2O_2Fe$
mol wt (g mol^{-1})	623.10	406.82	510.54	572.62	522.51	370.36	384.37	454.50	474.51	513.38	532.59	492.29
crystal system	monoclinic	orthorhombic	monoclinic	monoclinic	monoclinic	monoclinic	triclinic	orthorhombic	monoclinic	triclinic	monoclinic	orthorhombic
space group	$P2_1/c$ (#14)	*Pbcn* (#60)	$P2_1/n$ (#14)	$P2_1/n$ (#14)	$P2_1/c$ (#14)	$P2_1/n$ (#14)	$P\bar{1}$ (#2)	*Pnma* (#62)	$P2_1/c$ (#14)	$P\bar{1}$ (#2)	$P2_1/n$ (#14)	*Pnma* (#62)
crystal color	brownish green	dark green	orange	orange	orange	yellowish brown	red	brownish green	brownish green	brownish green	orange	purple
crystal size (mm)	0.2 × 0.15 × 0.05	0.2 × 0.2 × 0.15	0.2 × 0.15 × 0.1	0.08 × 0.08 × 0.01	0.2 × 0.2 × 0.1	0.2 × 0.2 × 0.05	0.3 × 0.1 × 0.1	0.1 × 0.1 × 0.03	0.3 × 0.3 × 0.06	0.1 × 0.1 × 0.03	0.5 × 0.3 × 0.1	0.2 × 0.2 × 0.1
a (Å)	16.416(3)	28.804(8)	12.562(3)	13.078(5)	13.177(3)	9.957(2)	9.257(7)	17.646(3)	11.583(3)	8.696(2)	11.626(3)	16.603(3)
b (Å)	14.519(2)	10.617(3)	14.724(3)	13.533(4)	12.491(3)	11.791(3)	10.883(7)	14.518(3)	13.746(3)	9.286(3)	14.076(3)	13.690(3)
c (Å)	16.745(3)	14.556(4)	15.912(3)	18.648(7)	16.988(3)	17.630(4)	12.182(8)	9.5866(16)	17.565(4)	17.219(5)	18.009(4)	11.323(2)
α (deg)							101.044(6)			76.553(12)		
β (deg)	118.479(2)		107.457(4)	108.835(7)	99.092(3)	90.031(3)	110.649(3)		105.828(3)	84.382(19)	99.585(3)	
γ (deg)							109.369(8)			80.048(15)		
V (Å^3)	3508.0(10)	4451.6(20)	2807.5(11)	3123.8(19)	2760.9(10)	2069.8(9)	1015.1(12)	2405.1(7)	2690.8(10)	1329.6(7)	2906.0(12)	2573.6(8)
Z	4	8	4	4	4	4	2	4	4	2	4	4
ρ_{calc} (g cm^{-3})	1.180	1.214	1.208	1.217	1.257	1.188	1.257	1.255	1.171	1.260	1.217	1.270
μ(Mo Kα) (cm^{-1})	5.32	8.03	5.58	5.09	5.72	7.31	7.50	7.27	5.80	6.64	5.44	6.11
$2\theta_{max}$ (deg)	55.0	54.9	55.0	55.0	55.0	55.0	55.0	55.0	55.0	55.0	55.0	54.9
no. of measured rflns	28704	33813	22156	25082	21777	23783	7993	2850	21302	10735	22481	20127
no. of observns data[a]	5273	5042	6240	6817	6214	4695	4362	2019	5821	5660	6459	3058
no. of Variables	379	261	358	405	363	281	260	170	301	304	373	200
R^b	0.045	0.041	0.040	0.053	0.034	0.082	0.030	0.028	0.069	0.050	0.039	0.056
Rw^c	0.057	0.056	0.067	0.078	0.051	0.108	0.047	0.039	0.123	0.074	0.058	0.071
GOF[d]	1.11	1.05	1.01	1.24	1.01	1.44	1.01	1.02	1.29	1.39	1.00	1.09

[a] Obsevation $I > 2\sigma(I)$. [b] $R = \Sigma||F_o|-|F_c||/\Sigma|F_o|$. [c] $Rw = [\{\Sigma w(|F_o|-|F_c|)^2\}/\Sigma wF_o^2]^{1/2}$. [d] $GOF = [\{\Sigma w(|F_o|-|F_c|)^2\}/(N_o - N_p)]^{1/2}$, where N_o and N_p denote the number of data and parameters.

Coupling of Heterocycles with Catecholborane Mediated by 6. (a) Thiophene: A yellowish-brown solution of **6** (0.065 mmol) was prepared by dissolving red crystals of **7** (25 mg) and hexamethylbenzene (12 mg, 0.074 mmol, as internal standard) in THF (1.5 mL) under an argon atmosphere. To this solution was added thiophene (12 μL, 0.15 mmol) at room temperature. After stirring for 1 h, a THF solution of catecholborane (31 mg, 0.26 mmol) was added dropwise into the reaction flask. The solvent was removed under reduced pressure, and the residue was dissolved in C_6D_6 (0.6 mL). The ^{1}H NMR spectrum of the resultant purple solution exhibited sets of signals for 2-(catecholboryl)thiophene and Cp*Fe(L^{iPr})(H_2Bcat) (**14**, see below) in 75% and 59% yields, respectively, based on the internal standard. (b) Furan: In a similar manner, the reaction of **6** (0.062 mmol) with furan (10 μL, 0.14 mmol) and catecholborane (33 mg, 0.28 mmol) in THF (1.5 mL) yielded 2-(catecholboryl)furan and **14** in 90% and 79%, respectively. (c) Benzothiophene: The reaction of **6** (0.070 mmol) with benzothiophene (39 mg, 0.29mmol) and catecholborane (42 mg, 0.35 mmol) in THF (0.6 mL) yielded 2-(catecholboryl)benzothiophene and **14** in 83% and 43%, respectively. (d) Benzofuran: The reaction of **6** (0.47 mmol) with benzofuran (6 μL, 0.054 mmol) and catecholborane (23 mg, 0.19 mmol) in C_6D_6 (1.5 mL) yielded 2-(catecholboryl)benzofuran and **14** in 62% and 10%, respectively. The coupling products were characterized by comparison of the NMR signals with those of authentic samples, which were prepared from 2-aryl-boric acid and catechol. See Supporting Information for details on synthesis and characterization.

Synthesis of Cp*Fe(L^{iPr})(H_2Bcat) (14). A yellowish-brown solution of **6** (0.17 mmol) was prepared by dissolving red crystals of **7** (65 mg) in toluene (3 mL) under an argon atmosphere. To this solution was added furan (14 μL, 0.19 mmol) at room temperature with stirring for 1 h. To this mixture was added a toluene solution (3 mL) of catecholborane (89 mg, 0.74 mmol) via syrringe. The solvent was removed under reduced pressure, and the resulting solid was washed with hexane (5 mL). The residue was extracted with toluene (15 mL) and centrifuged. The solution was concentrated to *ca.* 5 mL, and cooled at −30 °C to give Cp*Fe(L^{iPr})(H_2Bcat) (**14**, 27 mg, 32% yield) as purple crystals. ^{1}H NMR (C_6D_6): δ 7.11 (d, J = 7.6 Hz, 1H, Bcat), 6.73 (dd, J = 7.6, 7.6 Hz, 1H, Bcat), 6.67 (d, J = 7.6 Hz, 1H, Bcat), 6.63 (dd, J = 7.6, 7.6 Hz, 1H, Bcat), 6.19 (sept, J = 6.9 Hz, 2H, ^{i}Pr), 1.92 (s, 15H, Cp*), 1.70 (s, 6H, $CN_2C_2\mathit{Me}_2$), 1.37 (d, J = 6.9 Hz, 6H, ^{i}Pr), 1.10 (d, J = 6.9 Hz, 6H, ^{i}Pr), −15.6 (br, $w_{1/2}$ = 205 Hz, 2H, Fe−H−B). ^{11}B{^{1}H} NMR (C_6D_6): δ 35.9 ($w_{1/2}$ = 220 Hz). ^{13}C{^{1}H} NMR (C_6D_6): δ 198.7 ($\mathit{C}N_2C_2Me_2$), 154.3 (Bcat), 153.3 (Bcat), 126.3 ($CN_2\mathit{C}_2Me_2$), 120.3 (Bcat), 120.1 (Bcat), 82.9 (C_5Me_5), 53.7 (^{i}Pr), 23.5 (^{i}Pr), 21.2 (^{i}Pr), 12.2 ($C_5\mathit{Me}_5$), 11.3 ($CN_2C_2\mathit{Me}_2$). Anal. Calcd for $C_{27}H_{41}BN_2O_2Fe$: C, 65.88; H, 8.40; N, 5.69. Found: C, 66.08; H, 8.27; N, 5.54.

Thermodynamic Studies of the Reactions of 6 with Heteroarenes. Equilibrium constants between heteroaryl complexes and **6**+heteroarenes were obtained from K_1∼K_4 in the formulas below.

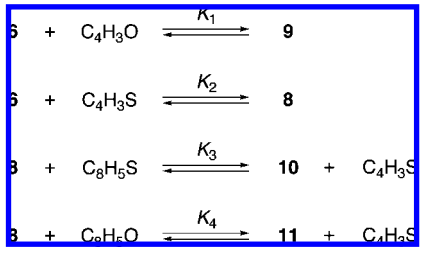

Determination of K_1: A solution of **6** (0.034 mmol) was prepared by dissolving red crystals of **7** (13 mg) in a 0.28 M cyclohexane (internal standard) solution of C_6D_6 (0.6 mL) under an argon atmosphere. To this solution was added furan (2.5 μL, 0.034 mmol) in an NMR tube. The sample was heated in an oil bath, and ^{1}H NMR spectra were recorded periodically until the ratios of signals did not change. The equilibration of **6**, furan, and **9** was measured in the range of 40−70 °C. Based on the concentrations of **6**, **9** and furan determined by integration relative to the internal standard (cyclohexane), the equilibrium constants K_1 were determined as 667 L/mol (40 °C), 634 L/mol (45 °C), 468 L/mol (50 °C), 379 L/mol (55 °C), 299 L/mol (60 °C), 250 L/mol (65 °C), and 200 L/mol (70 °C). Determination of K_2: In a similar manner as described above, thiophene (3.5 μL, 0.044 mmol) was added to a 0.28 M cyclohexane solution of C_6D_6 (0.6 mL) containing **6** (0.044 mmol). The equilibration of **6**, thiophene, and **8** was measured in the range of 40∼70 °C. The equilibrium constants K_2 were determined as 2.24 × 10^3 L/mol (40 °C), 1.77 × 10^3 L/mol (45 °C), 1.16 × 10^3 L/mol (50 °C), 908 L/mol (55 °C), 741 L/mol (60 °C), 587 L/mol (65 °C), and 479 L/mol (70 °C). Determination of K_3: Equilibrium was attained in a similar manner, using a C_6D_6 solution of **10** (11 mg, 0.022 mmol) with thiophene (2.0 μL, 0.025 mmol). The equilibrium constants K_3 were determined as 15.2 (40 °C), 13.5 (45 °C), 12.4 (50 °C), 11.8 (55 °C), 11.2 (60 °C), 10.5 (65 °C), and 9.97 (70 °C). Determination of K_4: Equilibrium was attained in a similar manner, using a C_6D_6 solution of **11** (5 mg, 0.010 mmol) with thiophene (1.0 μL, 0.012 mmol). The equilibrium constants K_4 were determined as 15.0 (40 °C), 12.8 (45 °C), 11.8 (50 °C), 11.4 (55 °C), 10.5 (60 °C), 9.02 (65 °C), and 7.90 (70 °C). The enthalpy and entropy parameters were calculated from a Van't Hoff plot (Figure 8 and Supporting Information).

X-Ray Crystal Structure Determination. Crystal data and refinement parameters for **2a**−**3b**, **5**−**10**, **13a**, and **14** are summarized in Table 2. Preliminary crystallographic results for **4** and **11** are given in the Supporting Information. Single crystals were coated with oil (Immersion Oil, type B: Code 1248, Cargille Laboratories, Inc.) and mounted on loops. Diffraction data were collected at −100 °C under a cold nitrogen stream on a Rigaku AFC7R equipped with a Mercury CCD detector, on a Rigaku AFC8 equipped with a Saturn70 CCD detector, or on a Rigaku FR-E equipped with a Saturn70 CCD detector using graphite-monochromated Mo Kα radiation (λ = 0.710690 Å). Six preliminary data frames were measured at 0.5° increments of ω, to assess the crystal quality and preliminary unit cell parameters. The intensity images were also measured at 0.5° intervals of ω. The frame data were integrated using the CrystalClear program package, and the data sets were corrected for absorption using a REQAB program. The calculations were performed with the CrystalStructure program package. Whereas β for **6** is nearly 90° and is suggestive of an orthorhombic crystal system, crystallographic C_s symmetry required for the indicated space group *Pnma* does not fit with the structure. Instead, the structure of **6** was determined based on monoclinic, $P2_1/n$. Whereas the CIF-check program performed on **9** suggests the higher symmetry, the systematic absences required for the indicated space group $C2/m$ do not fit with the diffraction data. The number of extinctions having an $I/\sigma(I)$ greater than 3.0 was 1898. Thus the structure was solved based on $P2_1/c$. All structures were solved by direct methods, and refined by full-matrix least-squares. Anisotropic refinement was applied to all non-hydrogen atoms except for disordered groups in **6**, **9**, and **10** (refined isotropically), and all hydrogen atoms were put at calculated positions. The cyclometalated L′^{iPr} ligand and iron in **6** are disordered over two positions, with occupancy factors of 50:50. The crystal solvent (pentane) and Cp* in **9**·1/2C_5H_{12} are disordered over two positions, with occupancy factors of 50:50. The 2-benzothienyl ligand and Cp* in **10** are disordered over two positions, with occupancy factors of 50:50. Additional data are available as Supporting Information.

Acknowledgment. This research was financially supported by Grant-in-Aids for Scientific Research (Nos. 18GS0207 "Organometallic and Cluster Chemistry in Metalloenzymes with Reducing Activities" and 18064009 "Synergy of Elements") from the Ministry of Education, Culture, Sports, Science and Technology, Japan. We

thank Roger E. Cramer at the University of Hawaii for fruitful discussion and careful reading of the manuscript.

Supporting Information Available: X-ray crystallographic information file for the structures of **2a**-**3b**, **5**-**10**, **13a**, and **14** (CIF), molecular structures and selected bond distances and angles for complexes **2b**, **3a**, **5**, **9**, and **13a**, preliminary results on X-ray analysis of **4** and **11**, details on thermodynamic studies, and the synthesis and characterization of 2-(catecholboryl)arenes (PDF). This material is available free of charge via the Internet at http://pubs.acs.org.

JA8063028